IEEE Access
Multidisciplinary | Rapid Review | Open Access Journal

Received September 30, 2021, accepted October 19, 2021, date of publication October 22, 2021, date of current version November 3, 2021.

Digital Object Identifier 10.1109/ACCESS.2021.3122181

Recent Advancements in Quasi-Isotropic Antennas: A Review

SYED IMRAN HUSSAIN SHAH[1], SONAPREETHA MOHAN RADHA[1], (Student Member, IEEE), PANGUN PARK[2], (Member, IEEE), AND ICK-JAE YOON[1], (Senior Member, IEEE)

[1]Department of Electrical Engineering, Chungnam National University, Daejeon 34134, Republic of Korea
[2]Department of Radio and Information Communications Engineering, Chungnam National University, Daejeon 34134, Republic of Korea

Corresponding author: Ick-Jae Yoon (ijyoon@cnu.ac.kr)

This work was supported in part by the Basic Research Laboratory (BRL) of the National Research Foundation under Grant NRF-2020R1A4A2002021 funded by the Government of Korea, and in part by the Institute of Information and Communications Technology Planning and Evaluation (IITP) funded by the Government of Korea (MSIT, Development of Advanced Power and Signal EMC Technologies for Hyper-Connected E-Vehicle) under Grant 2020-0-00839.

ABSTRACT Quasi-isotropic antennas are promising candidates due to their applications in modern communication systems, where full spatial coverage and/or uniform signal reception is required. In this work, an in-depth review of quasi-isotropic antennas is presented, with the aim of understanding the working principles of such antennas and presenting the recent advancements, challenges, and solutions offered by various researchers. First, different design techniques adopted to achieve quasi-isotropic patterns, such as the use of complementary dipoles, multiple monopoles or dipoles, and an array of discrete elements are discussed. Then, different types of quasi-isotropic antennas—for example, planar, electrically small, 3-D printed, dual-band/wideband, circularly polarized, metamaterial-inspired, and dielectric resonator-based quasi-isotropic antennas—are revisited. Their applications in various technologies, such as RFID, energy harvesting, wireless sensor networks, and the IoT, are briefly explained. Lastly, different key performance parameters, such as complexity of configuration, design approach, physical profile, far field and radiation characteristics, reflection coefficients, operating frequency and bandwidth, gain deviation, and fabrication process, are discussed and tabulated. This review not only provides a guideline but will also help antenna engineers in designing a quasi-isotropic antenna with desirable performance.

INDEX TERMS Quasi-isotropic antennas, gain deviation, electric dipole, magnetic dipole, metamaterials.

I. INTRODUCTION

Wireless networks are a cost-effective and scalable alternative to cable networks for a wide range of applications, as using cables in complex control environments presents prohibitive costs and practical difficulties. Their simplicity in deployment, low installation costs, and ease of operation and monitoring make wireless networks highly attractive in modern communication systems. Wireless networks are now considered a crucial infrastructure in industries for mission-critical control systems, such as automation, monitoring, power grid protection, IoT devices, and many more. In such situations, instability, or interruption in communication links can have a substantial impact on the performance of the system. Therefore, it is crucial to maintain stable connectivity of the network all the time, regardless of the orientation of the transmitter and receiver.

To date, several techniques have been employed to ensure stable connectivity in the entire region. A beam-scanning antenna array system may be used; however, it usually takes a large footprint and increases complexity. A more practical solution involves designing an antenna that can radiate electromagnetic energy equally in all directions with no radiation nulls in the space, which is also called an isotropic antenna [1]. Isotropic antennas that can provide full spatial coverage are currently fictional and cannot be realized theoretically. This is because the transverse electric field in the far field region cannot be uniform over a sphere if the field is linearly polarized everywhere [2], [3]. However, scientists have proposed null-free quasi-isotropic antennas [4].

Due to their isotropic-like characteristics, quasi-isotropic antennas can be very useful for several modern wireless communication technologies, such as IoT applications,

The associate editor coordinating the review of this manuscript and approving it for publication was Diego Masotti.

FIGURE 1. Scenarios requiring quasi-isotropic antennas (adapted from [5]–[7] and google images).

monitoring purposes, wearable gadgets, wireless power transfer, wireless sensor networks, wireless access points, intra-vehicle wireless communication, and radio frequency energy harvesting. Fig. 1 pictorially depicts various applications of quasi-isotropic antennas.

It is worth mentioning that gain deviation is the key parameter in evaluating quasi-isotropicity of an antenna. Gain deviation refers to the difference between the maximum and minimum gain values of an entire radiation sphere. An ideal isotropic antenna will have a zero-gain deviation because it radiates perfectly equally in all directions.

An alternative way is to calculate the integral isotropy factor, which can be determined by finding the ratio of the surface on which the gain deviation exceeds the threshold gain level, TH_{iso}, over the entire sphere surrounding the antenna [29], [61]. Radiation pattern isotropy is defined as the sum of the solid angles formed by radiation pattern beams whose gain lies between the peak gain (PG) and the TH_{iso} below the PG relative to a closed spherical surface surrounding the antenna. Mathematically, this can be described by the integral parameter I^{th-iso} presented in equation (1).

$$I^{th-iso} = 100\% \times \iint_{s1} \frac{sin\theta d\theta d\varphi}{4\Pi} \tag{1}$$

The S_1 surface is determined by

$$S_1, \text{ such that } PG - TH_{iso} \leq Gain\,(\theta, \varphi) \leq PG$$

However, there is no standard definition for the maximum gain deviation value yet. In the reported literature the gain deviation varies with respect to the operational characteristics of the antenna. For instance, from Table 1, II, and III we can see maximum gain deviation of single band antennas in planar and non-planar configurations are reported as 6.84 [30] and 7.9 dB [3] respectively. Similarly, for dual band antennas the maximum gain deviation has been reported as 8.9 and 9.9 dB, for each resonance, respectively [31], whereas for wideband antennas the reported gain deviation is around 6 dB [24]. The reported gain deviation for the circularly polarized antenna is 3.6 dB [32]. In the last decade, several studies have been presented to design quasi-isotropic antennas to minimize gain deviation [2], [3], [7], [8], [10], [13]–[24], [2], [3], [7], [8], [10], [13]–[24], [29], [31]–[53].

Different design approaches, such as split-ring resonators (SRR)-based antennas [17], electrically small antennas [10], [18], [35], [36], 3-D printed antennas [25], [30], [38], [54], planar antennas [23], [24], [36], dielectric resonator antennas [3], [14], and shorted patch antennas [15], [16], have been used to minimize gain deviation. Quasi-isotropic antennas based on some other techniques have also been reported like by folding dipole [8]–[12], magnetic dipole [13] and by symmetrically stacked planar antenna configurations [2], [28]. Figure 2, categorizes the different approaches for designing quasi-isotropic antennas. However, due to the design complexity and feeding mechanism, these techniques are not very common and only few antennas have been designed using these techniques. Antennas with quasi-isotropic characteristics can also be divided into different categories based on their operational characteristics, as shown in Fig. 3.

Depending on their geometric configurations, quasi-isotropic antennas can be classified as planar and non-planar, as depicted in Fig 4. So far classification in terms of designing is concerned, an intuitive way is to combine two orthogonal electric and magnetic dipoles [2], [10], [13]–[18]. The orthogonal horizontal and vertical dipoles have omnidirectional radiation patterns in the vertical and horizontal planes, respectively, as shown in Fig. 5. Therefore, a quasi-isotropic radiation pattern is achieved when two perpendicular complementary dipoles are excited with quadrature signals of equal amplitude. This concept was first employed in [33] and [34] by combining linear and slot antennas. In [34], a combination of a slot antenna and a linear dipole antenna was presented to obtain a quasi-isotropic pattern. The slot and dipole can be arranged in three orthogonal orientations, providing desirable performance in terms of quasi-isotropic coverage [34]. First, when the dipole antenna is kept parallel to both the slot and the plane of the slot, it results in circular polarization over a wide range. Secondly, when the dipole is placed parallel to the plane of the slot but perpendicular to the slot itself, maximum coupling is achieved, and both antennas react as a conventional two-element array of parallel dipoles. The third orientation of the dipole is interesting in the way that when the dipole is placed perpendicular to both the slot and the plane of the slot, both antennas completely decouple, and their mutual independent fields superimpose to achieve the total field. This approach can be used to achieve quasi-isotropic radiation patterns in phased array antennas [33]. This concept has also been used to realize a dielectric resonator-based quasi-isotropic antenna [14].

The second way to design a quasi-isotropic antenna is to use an array of discrete elements in a circular fashion to cover nearly isotropic region. Several antenna designs employing this approach have been reported [19]–[21]. However,

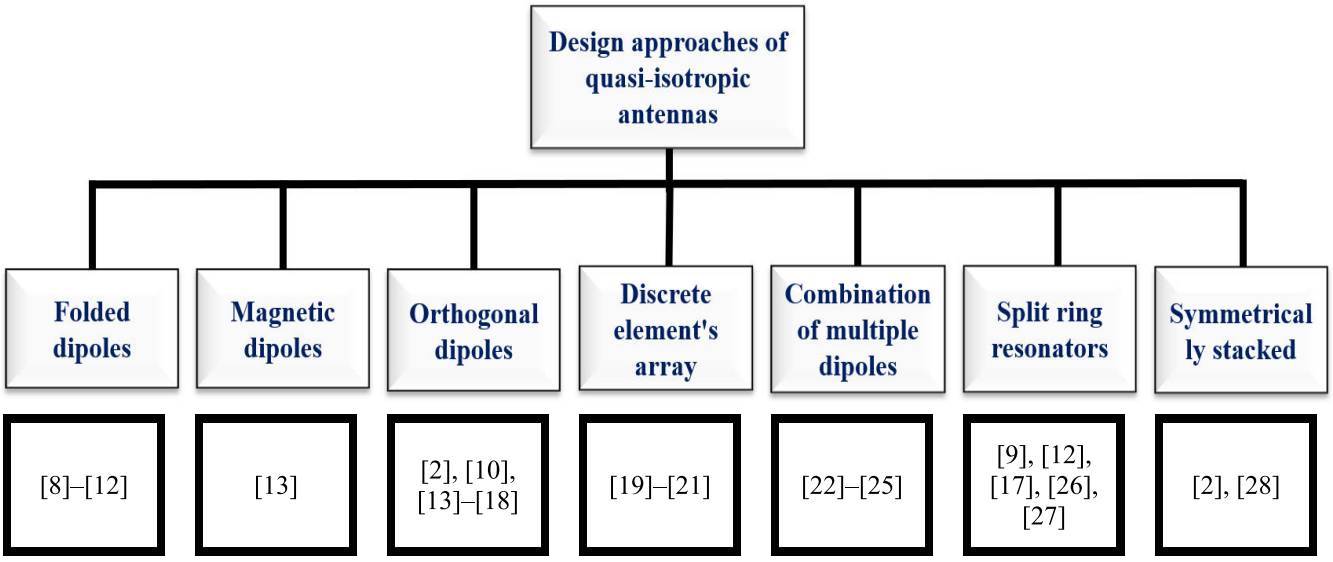

FIGURE 2. Classification of quasi-isotropic antennas based on design approaches.

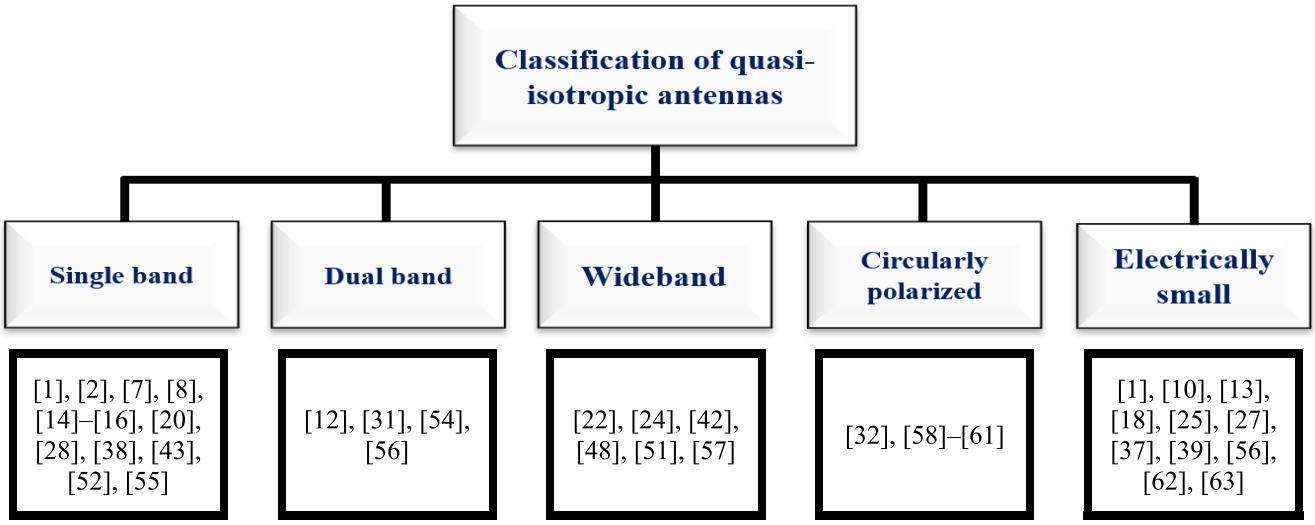

FIGURE 3. Classification of quasi-isotropic antennas based on operational characteristics.

antennas designed using this technique are bulky, large in size, and require a complex feeding network. The third way to design quasi-isotropic antennas is to use multiple electric monopoles, electric dipoles, or magnetic dipoles to achieve quasi-isotropic radiation coverage. This procedure has been employed in many designs [22]–[25].

This article presents a detailed analysis and in-depth review of different types of quasi-isotropic antennas that can provide full spatial coverage with minimum gain deviation. It also discusses the implementation of different design techniques to achieve a quasi-isotropic pattern, including a tabulated detailed performance comparison between different techniques. The purpose of this article is to provide a guideline to the research community for designing a quasi-isotropic antenna with the desired specifications and performance.

This paper is arranged as follows: Section II presents theory and well-known design approaches for different types of quasi-isotropic antennas. Section III presents state-of-the-art quasi-isotopic antennas.

Section IV presents applications and Section V presents some challenges and future directions. Lastly, the concluding remarks are presented in Section VI.

II. DESIGN APPROACHES FOR QUASI-ISOTROPIC ANTENNAS

A. COMBINATION OF ELECTRIC AND MAGNETIC DIPOLE

The intuitive way to obtain the quasi-isotropic radiation pattern is to use two orthogonal magnetic dipoles [13], two orthogonal electric dipoles [23], or orthogonal electric and equivalent magnetic dipoles [14], [15], [17]. According to the

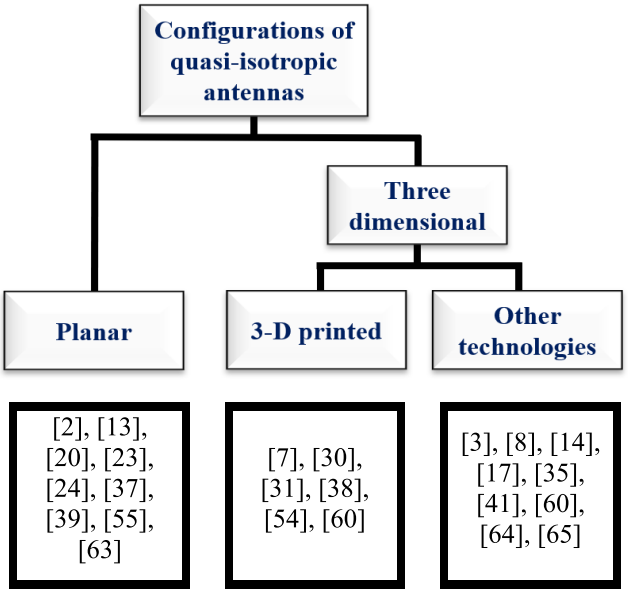

FIGURE 4. Classification of quasi-isotropic antennas based on geometry.

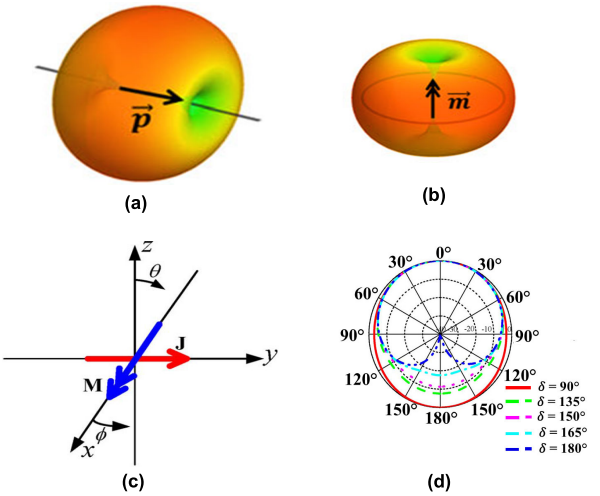

FIGURE 5. (a) Radiation pattern of an electric dipole, (b) radiation pattern of a magnetic dipole [17], (c) configuration of the orthogonal electric and magnetic dipoles, (d) elevation patterns of the complementary dipoles for different values of φ [14].

concept of complementary dipoles [2], [3], [14], when two equivalent dipoles are fed with two signals of the same amplitude and quadrature phase, the maximum-field direction of the one is along the null-field direction of the other one. This is due to the generation of omnidirectional radiation patterns by dipoles that are in perpendicular planes with each other. As a result, the directions of the weak power density can be strengthened, and the blind spot can be minimized. Hence, nearly full spatial signal coverage can be obtained.

Fig. 5 (c) depicts the antenna configuration, which consists of a pair of orthogonal electric and magnetic dipoles aligned with the y-axis and x-axis, respectively. By superimposing the far fields of complementary antennas, the overall far fields

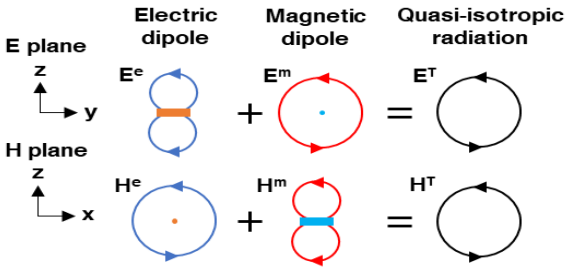

E^e, H^e: Electric and Magnetic fields of a y-directed electric dipole.
E^m, H^m: Electric and Magnetic fields of an x-directed magnetic dipole.
E^T, H^T: Resultant electric and Magnetic fields of complimentary dipoles.

FIGURE 6. The basic principle of complementary dipole-based quasi-isotropic antenna [3].

can be obtained [33]. The E-fields of the x-directed magnetic dipole (denoted by $E_{m\theta}$ and $E_{m\phi}$) is given by (1) to (4) [14]:

$$E_{m\theta} = jI_m l_m F_m sin\phi \tag{2}$$
$$E_{m\phi} = jI_m l_m F_m cos\theta cos\phi \tag{3}$$
$$E_{e\theta} = -jI_e l_e F_e cos\theta sin\phi \tag{4}$$
$$E_{e\phi} = -jI_e l_e F_e cos\phi \tag{5}$$

where;

$$F_m = (\beta/4\pi r)e^{j\omega[t-(r/c)]}$$
$$F_e = (\eta\beta/4\pi r)e^{j\omega[t-(r/c)]}$$

The fields of the magnetic dipole are deduced from the results of a small electric loop for a magnetic moment of $E_{m\theta} = I_m l_m = j\omega\mu IS$ [66]. The components of the total field can be obtained if the phase difference between the two sources is φ (say).

$$E_\theta^T = E_{e\theta} + E_{m\theta} = -jI_e l_e F_e cos\theta sin\phi + e^{j\varphi} jI_m l_m F_m sin\phi \tag{6}$$
$$E_\phi^T = E_{e\phi} + E_{m\phi} = -jI_e l_e F_e cos\phi + e^{j\varphi} jI_m l_m F_m cos\theta cos\phi \tag{7}$$

Suppose $\eta I_e l_e = I_m l_m$, or equivalently, $\eta = {I_m l_m}/{I_e l_e}$
The total field E_T is then given by:

$$E_T = \sqrt{|E_\theta^T|^2 + |E_\phi^T|^2} = IlF\sqrt{1 + \cos^2\theta - 2cos\theta cos\varphi} \tag{8}$$

Apparently, E_T is a function of θ *and* φ only, and independent of azimuthal angle ϕ, revealing that the field is omnidirectional in the azimuthal plane [14]. The radiation patterns for the different values of phase difference (φ), for the elevation field of combined complementary dipoles are shown in Fig. 5(d). The complementary theory is pictorially elucidated in Fig. 6 [3].

Based on the complementary dipole technique, different types of quasi-isotropic antennas, such as non-planar and planar, electrically small antennas, shorted patch antennas, folded split-ring resonators, and dielectric resonator

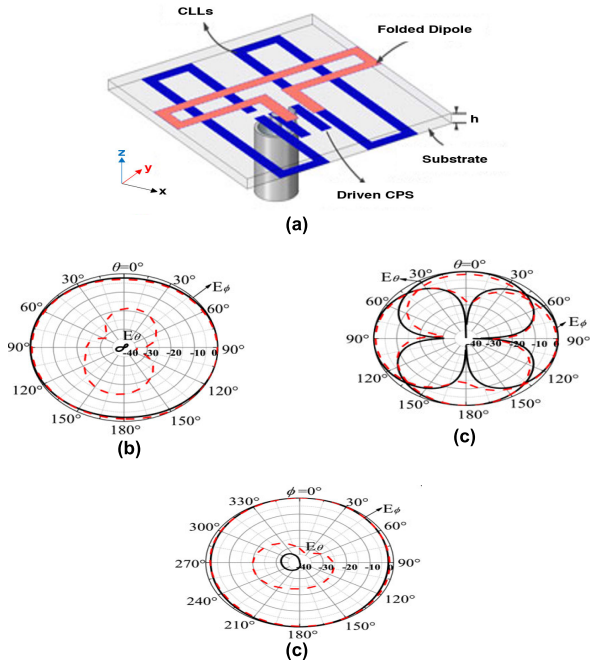

FIGURE 7. Electrically small planar antenna, (a) perspective view, (d) xz plane, (e) yz plane, (f) xy plane [10].

antennas, have been reported in the literature [2], [3], [10], [13]–[18], [37]. A planar, electrically small antenna as shown in Fig. 7, with a quasi-isotropic radiation pattern was reported in [10].

B. METHOD OF USING THE ARRAY OF DISCRETE ELEMENTS ON CONDUCTING LOOPS

Quasi-isotropic antennas can also be designed using a circular array of discrete elements. The common approach for obtaining nearly isotropic patterns using this method is to use discrete antenna arrays along the circumference of a cylinder [19]–[21], [40], [41]. However, this approach involves unavoidably bulky antenna designs and complex feeding networks. A conformal cylindrical array was proposed in [67], and it was found that some of the conformal cylindrical antenna structures proposed in the literature have omnidirectional direction patterns in some planes but not with full spherical coverage [59], [61], [68]–[70].

In another study [20], a low-profile, tri-polarized planar quasi-isotropic antenna was proposed for 2.4-2.5 GHz. The antenna had three layers, where the top and bottom layers were composed of dielectric material with a similar thickness, while an air layer was incorporated between them.

A dual-polarized circular patch was designed on the top side of the upper substrate, whereas two orthogonal feed lines were designed on the bottom side of the lower substrate, and the top side of the lower substrate contained ground plane. The ring patch of the top substrate was excited by etching a pair of H-shaped slots in the ground plane. Since the three ports of the antenna independently worked in three different modes, the radiating electric fields were excited

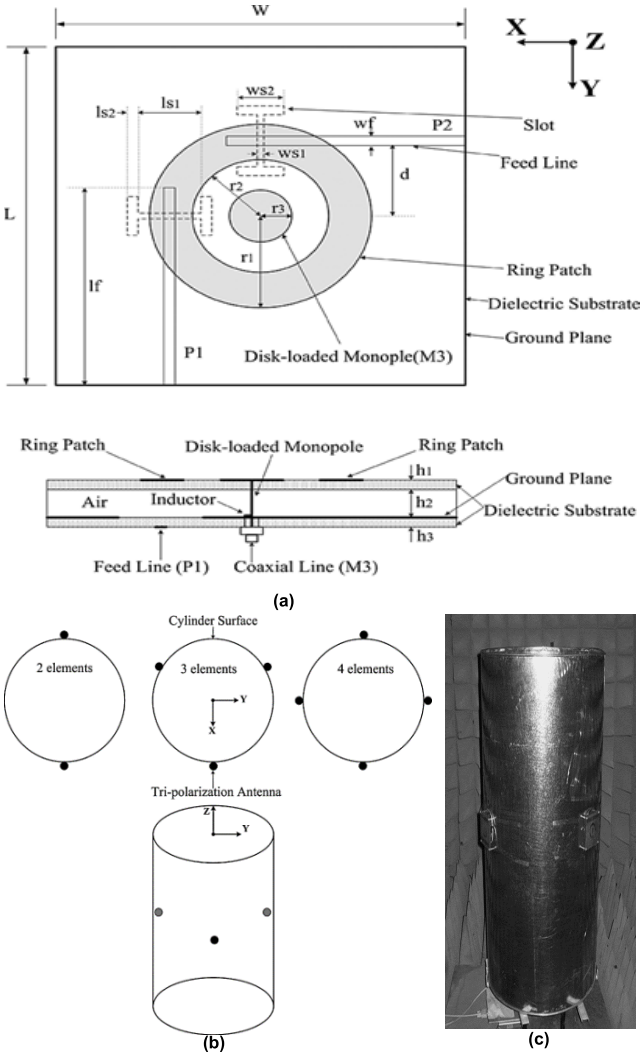

FIGURE 8. An example of an array of discrete elements to realize quasi-isotropic antenna (a) antenna geometry [20], (b) antenna element arrangement on cylindrical surface, (c) designed prototype [19].

by patch modes and were parallel to the x- and y-axes, as shown in Fig. 8(a). Moreover, the electric field excited by the monopole was parallel to the z-axis. The presented design on the surface of a conducting cylinder in different combinations is shown in Fig. 8(b), and the final prototype is depicted in Fig. 8(c). Collectively, the antenna radiated three orthogonal polarized fields. The measured −6 dB impedance bandwidths for the three ports were 2.34–2.54 GHz, 2.35–2.52 GHz, and 2.38–2.49 GHz, respectively. The isolation between the three ports was also better than −24 dB. In summary, the proposed tri-polarized antenna can be used with each port to transmit independent signals.

Similarly, in [19], another conformable switchable antenna was presented, whose basic element structure is based on the design presented in [20]. Full spatial coverage was obtained by switching among the three tri-polarized antennas over the complete spherical region. The proposed antenna was low profile and easy to integrate on cylindrical surfaces.

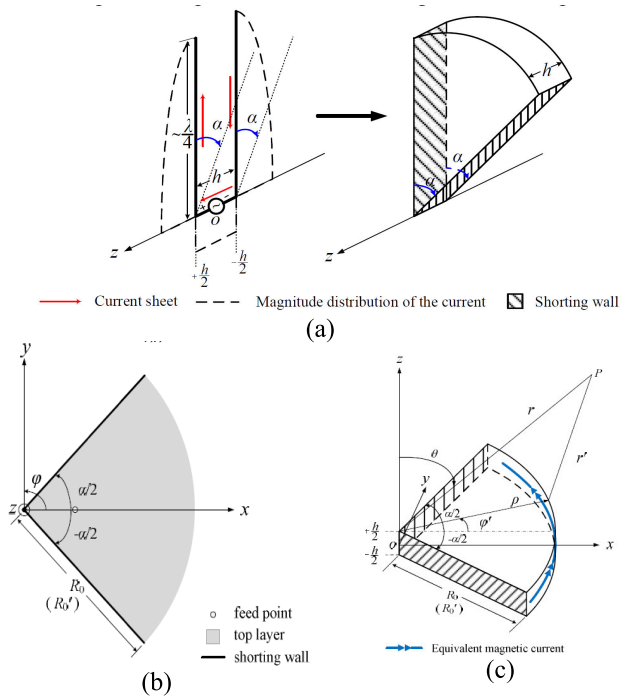

FIGURE 9. Evolution of proposed planar quasi-isotropic antenna: (a) evolution process, (b) top view, (c) cavity model [13].

As the three ports of this antenna radiated orthogonal polarized fields, it could receive signals with any polarization, thus avoiding polarization mismatch. Furthermore, another extremely important feature of this type of antenna was the complementary radiation properties of the patch and monopole antenna mode. By switching among them, full radiation coverage for a hemisphere was obtained. Therefore, to realize a full coverage for the cylindrical antenna system, only two tri-polarization antennas are needed [19].

C. METHOD OF USING MAGNETIC DIPOLE

A U-shaped quarter-wavelength radiator current source which is an example of magnetic dipole can exhibit a near-isotropic radiation characteristic. Normally, it consists of two vertical arms spaced by about a quarter-wavelength separated by a short crosspiece that is far less than the operational wavelength.

The analysis is simplified by considering a centered-fed, U-shaped dipole with the approximate length of one quarter-wavelength in free space shown in Fig. 9(a) [13]. Suppose the short cross piece (with a length of h) is aligned with the z-axis. By rotating the two vertical arms to a certain angle with respect to the z-axis, the U-shaped quarter-wavelength dipole can be transformed into a planar antenna as shown in Fig.9 (a). The two vertical arms evolving into the top and bottom surfaces of the cavity, the short cross piece forms a shorting wall with a height of h. As a result, the linear, 1-D antenna becomes a cavity-like, 2-D antenna as shown in Fig. 9 (b) - (c). An antenna formed by the two sectors will exhibit the typical behavior of a magnetic current sheet on an aperture. An antenna can be modeled as a planar circular sector magnetic dipole, and the cavity model can be used to predict its radiation behavior rigorously.

When $h \to 0$, the fields inside a circular sector cavity can be determined by solving the wave equation. At the edge of the sector, and for the magnetic-wall boundary conditions to be satisfied, the radial surface current must vanish, such that,

$$J_\rho\left(\rho = R_0\right) = H_\varphi\left(\rho = R_0\right) = 0 \tag{9}$$

R_0 is the radius of the circular sector, whose value can be calculated using the first-order derivative of the Bessel function of order v

$$\begin{aligned} J_v' &= (\chi_{v1}) = 0 \\ R_0 &= \frac{\chi_{v1}}{k} = \frac{\chi_{v1} c}{2\pi f_0} \end{aligned} \tag{10}$$

where $v = n\pi/a$, n represents the number of circumferential variations, c is the speed of light, f_0 is the central frequency J_v' and χ_{v1} are the first-order derivatives of the v-order Bessel function respectively. For a very low height h, the radius of the circular sector can be slightly modified as that of low-profile antenna,

$$R_0 \cong R_0 - \frac{h}{2} = \frac{\chi_{v1} c}{2\pi f_0} - \frac{h}{2} \tag{11}$$

As $h \ll \lambda_0$, there is no variation along z-axis. Therefore, the electric field within the cavity has only a z-component, and magnetic field essentially has only ρ and φ components. The equivalent magnetic current aperture is given by:

$$\begin{aligned} \vec{M} &= \vec{P} \times \hat{\rho} = E_Z \hat{\varphi} \\ &= \begin{cases} \hat{\varphi} \sum_n^\infty E_v J_v(k\rho) \cos v\varphi, & v = \dfrac{n\pi}{\alpha},\ n = 1, 3, 5, \ldots \\ \hat{\varphi} \sum_n^\infty E_v J_v\left(k\rho\right) \sin v\varphi, & v = \dfrac{n\pi}{\alpha},\ n = 1, 3, 5, \ldots \\ R_0' \le \rho \le R_0' + \dfrac{h}{2} \end{cases} \end{aligned} \tag{12}$$

The radiation field can be obtained by integrating the far fields generated by the magnetic current along the circular sector from $-\alpha/2$ to $\alpha/2$. In this way, the E-field of the planar antenna can be calculated by analyzing its azimuthal components.

$$\begin{aligned} E_\theta = {} & \frac{-jk}{4\pi} \frac{e^{-jkr}}{r} \iint_{-\frac{\alpha}{2\rho}}^{\frac{\alpha}{2}} M_\varphi\left(\rho, \acute{\varphi}\right) \\ & \times \cos(\acute{\varphi} - \varphi) \times e^{[jk\rho \sin\theta \cos\varphi - \acute{\varphi}]} \rho d\rho d\acute{\varphi} \end{aligned} \tag{13}$$

$$\begin{aligned} E_\varphi = {} & \frac{-jk}{4\pi} \frac{e^{-jkr}}{r} \cos\theta \iint_{-\frac{\alpha}{2\rho}}^{\frac{\alpha}{2}} M_\varphi\left(\rho, \acute{\varphi}\right) \\ & \times \sin(\acute{\varphi} - \varphi) \times e^{[jk\rho \sin\theta \cos\varphi - \acute{\varphi}]} \rho d\rho d\acute{\varphi} \end{aligned} \tag{14}$$

Since a virtual, infinite electrical wall occurs at z = 0 based on the natural boundary condition of the cavity, so, the magnetic current should have an effective radial extent of

h/2 owing to the exponential decay of the electrical field for $\rho > R_0'$. Based on resonance approximation, the expressions for the components E_θ and E_φ can be simplified (considering only the non-static, fundamental mode) as follow:

$$E_\theta = \frac{-jk}{4\pi}\frac{e^{-jkr}}{r}R_0' hE_v J_v(\chi_{v1}) \int_{-\frac{\alpha}{2}}^{\frac{\alpha}{2}} \cos v\varphi' \times \cos(\acute{\varphi}-\varphi) \times e^{[jkR_0' \sin\theta \cos(\acute{\varphi}-\varphi]} d\acute{\varphi} \quad (15)$$

$$E_\varphi = \frac{-jk}{4\pi}\frac{e^{-jkr}}{r}R_0' hE_v J_v(\chi_{v1}) cos\theta \int_{-\frac{\alpha}{2}}^{\frac{\alpha}{2}} \cos v\varphi' \times \sin(\acute{\varphi}-\varphi) \times e^{[jkR_0' \sin\theta \cos(\acute{\varphi}-\varphi]} d\acute{\varphi} \quad (16)$$

where $hEvJv\ (\chi v1)$ is the edge voltage at $\varphi = 0$. The magnitude of the total field E_{total} is given by:

$$|E_{total}| = \sqrt{|E_\theta|^2 + |E_\varphi|^2} \quad (17)$$

When radius R_0' is determined, the total radiation pattern is only dominated by the flared angle α of the circular sector. The normalized total field pattern for three principle planes, i.e., $\varphi = 0°$ (the xz-plane), $\varphi = 90°$ (the yz-plane), and $\theta = 90°$ (the xy-plane) are theoretically predicted by using (15) - (17). This means that by changing the flared angle α we can adjust the uniformity of the antenna's radiation pattern since the uniformity of the radiation pattern is dominated by order v of the resonant cavity mode. It is observed that when $\alpha = 3\pi/2$, the total field patterns have non-uniformities less than 1dB, suggesting the antenna should have quasi-isotropic radiation patterns.

D. METHOD OF USING MULTIPLE MONOPOLES OR DIPOLES

Another way to design quasi-isotropic antennas involves the use of multiple monopoles or dipoles with planar as well as 3-D structures [22]–[25], [30], [31], [39], [54]. In [31], a dual-band wire antenna bent and wrapped on the surface of a package was proposed and fabricated using an additive manufacturing technique. The antenna was a dual band with quasi-isotropic radiation patterns and can be used for the GSM900 and GSM1800 bands. The radiation pattern of the wire antenna can be visualized as the superposition of the radiation patterns of a set of electrical dipoles. Each bent portion of the wire antenna was assumed to act as an electric dipole. The basic analysis model for the set of orthogonal electric dipoles is shown in Fig. 10. The current densities along the x-, y- and z- directions in the cartesian coordinates system can be expressed as:

$$J_x(x,y,z) = m_x \delta(x)\delta(y)\delta(z)x_o \quad (18)$$

$$J_y(x,y,z) = m_y \delta(x)\delta(y)\delta(z)y_o \quad (19)$$

$$J_z(x,y,z) = m_z \delta(x)\delta(y)\delta(z)z_o \quad (20)$$

where m_x, m_y, and m_z are the dipole moments along the x, y, and z axes, respectively, x_o, y_o, and z_o are the unit vectors along x-, y-, and z-axes, δ is the Dirac delta function, and

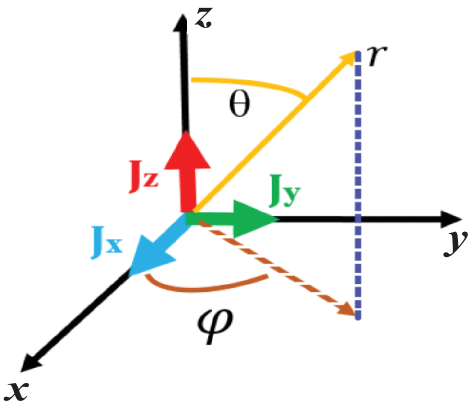

FIGURE 10. The basic model of an orthogonal set of x-, y-, and z-oriented electric dipoles [31].

J_x, J_y, and J_z are the current densities of the dipoles along the respective axes.

In spherical coordinates system (r, θ, φ), the electric dipole along the x-axis has the meridional component E_θ, and azimuthal component E_φ.

$$E_\theta(\theta,\varphi) = -j\eta cos\theta cos\varphi \frac{k}{4\pi} m_x \quad (21)$$

$$E_\varphi(\varphi) = j\eta sin\varphi \frac{k}{4\pi} m_x \quad (22)$$

Similarly, the components along the y-axis of the radiation pattern of the dipole are:

$$E_\theta(\theta,\varphi) = -j\eta cos\theta sin\varphi \frac{k}{4\pi} m_y \quad (23)$$

$$E_\varphi(\varphi) = -j\eta cos\varphi \frac{k}{4\pi} m_y \quad (24)$$

The radiation pattern of the z-oriented component has only a meridional component:

$$E_\theta(\theta) = j\eta sin\theta \frac{k}{4\pi} m_z \quad (25)$$

Thus, the total radiation pattern of the three orthogonal dipoles with unit vectors ($m_x, m_y, m_z = 1$), having a phase shift ψ_1 within x- and y-oriented dipoles and a phase shift ψ_2 within z- and x-oriented dipoles can be expressed as:

$$\left|E^{\Sigma}(\theta,\varphi)\right|^2 = \left(\eta\frac{k}{4\pi}\right)^2 \left(2 - \sin^2\theta \sin(2\varphi)\right) cos\psi - \sin(2\theta)\, cos\varphi cos\psi_2 - \sin(2\theta)\, sin\varphi \cos(\psi - \psi_2)). \quad (26)$$

where $\eta = 120\pi$, $k = \frac{2\pi}{\lambda}$.

When $\psi = \pi/2$, (25) can be simplified as:

$$\left|E^{\Sigma}(\theta,\varphi)\right|^2 = \left(\eta\frac{k}{4\pi}\right)^2 (2 - \sin(2\theta)\cos(\varphi - \psi_2)) \quad (27)$$

The variation of the field pattern from maximum to minimum and the null direction can be found using (27). It was

observed in [31] that as long as there was a phase difference of 90° between any two dipoles (either x-y, y-z or z-x oriented), the configuration of three orthogonal electric dipoles provided quasi-isotropic radiation pattern with gain deviation of 4.77 dB regardless of the phase of the third dipole. Moreover, the quasi-isotropic pattern can also be achieved by using only two orthogonal electric dipoles. By using (3) and (5), and expressing the total radiation pattern for $\psi = {}^{\pi}/_{2}$ as:

$$\left|E^{\Sigma}(\theta)\right|^2 = \left(\eta\frac{k}{4\pi}\right)^2\left(1+\cos^2\theta\right) \tag{28}$$

In [23], two crossed curved dipoles are designed on top side of a substrate to get a nearly full spatial coverage. The compact printed planar quasi-isotropic antennas can serve for 2.4 GHz wireless local area network (WLAN) applications. The lengths of the two curved dipoles can be adjusted to achieve an isotropic radiation pattern in the frequency range of 2.4–2.48 GHz. The design of the crossed dipole antenna, along with its quasi-isotropic radiation pattern, is depicted in Fig. 11. The lengths of the straight part of two dipoles are L_p, whereas the angles of the curved parts of two dipoles are $\alpha + \Delta\alpha$ and α-$\Delta\alpha$, respectively. The widths of the two dipoles are the same, defined as W_p, and the distance between two branches of a dipole is twice of P_o. L_f is the width of the connecting sections that connects a branch of one dipole to the other. The length and width of the substrate is L_s. The presented antenna had an impedance bandwidth of 270 MHz (2.26–2.53 GHz, 11%) and the gain deviation was lower than 6 dB over the full space.

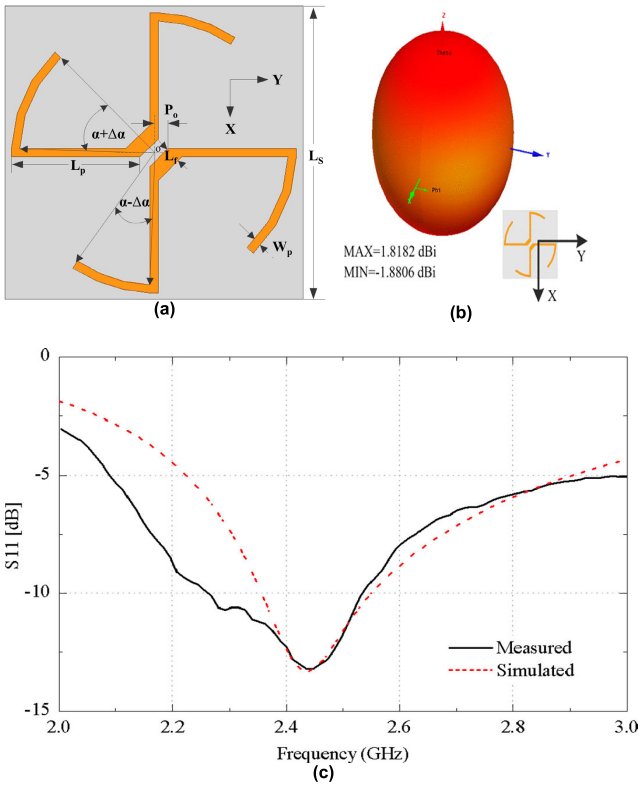

FIGURE 11. Isotropic antenna using two crossed dipoles (a) crossed dipole antenna configuration, (b) 3-D radiation pattern of the antenna, (c) the reflection coefficient [23].

III. STATE OF THE ART QUASI ISOTROPIC ANTENNAS

A. PLANAR QUASI-ISOTROPIC ANTENNAS

In modern wireless technology, planar antennas play an increasingly important role due to their nearly isotropic radiation pattern. In portable devices, such as mobile phones, tablets, laptops, and smart wrist watches, where profile, ease of installation, and cost are key performance constraints, planar antennas are used because these antennas are low profile, compatible with planar and non-planar surfaces, simple, mechanically robust, inexpensive to manufacture using advanced printed circuit technology, and very versatile in terms of resonance. Various quasi-isotropic antennas in planar configuration are proposed in [2], [13], [20], [23], [24], [37], [39], [55], [63].

Quasi-isotropic radiation characteristics were achieved using a planar folded dipole antenna in [55]. The design was based on a triple current line source. The spatial distance between these sources was optimized, providing phase differences to achieve a quasi-isotropic radiation pattern. The antenna consisted of three current elements fed by a single-port coaxial cable, as shown in Fig. 12. The current pairs I and II supported the quarter wavelength mode, while current III was almost uniform. A matching network comprising a capacitor and a pair of inductors was introduced for matching purpose. These current sources with known modes and current distributions made this design an efficient and favorable choice for practical implementation. In full space, the simulated and measured gain deviations were less than 3 dB and 6 dB, respectively, for the frequency range of 0.83 GHz to 1.06 GHz.

In another study [13], a circular centered-fed quarter-wavelength magnetic dipole antenna was used to achieve quasi-isotropic coverage, as depicted in Fig. 13. The U-shaped antenna can be modified to a planar antenna if both vertical arms are rotated to a specific angle α in the z-axis. The radiation pattern of the resulting antenna was dominated by the corresponding magnetic sheet of current on the aperture created by the two-sector surfaces. The antenna can then be treated as a magnetic dipole with a planar circular field. Within the three major planes, the antenna shows a better non-uniformity of lower than 5.7 dB and an average radiation efficiency of more than 82% within 2.4 GHz to 2.5 GHz. A planar angled dipole antenna with two parasitic radiating elements was reported in [39]. The parasitic elements were used to alter the near field and to help in improving the isotropy. This antenna system was designed at 2.4 GHz and provided an efficiency of almost 90% with a gain variation of 2 dB. A brief summary of the various planar quasi-isotropic antennas is presented in Table 1. Different key performance parameters, such as operating frequencies, fractional bandwidth, electrical size, and gain deviation are given.

TABLE 1. Summary of the planar quasi-isotropic antennas with their respective parameters and adopted techniques.

Ref.	Design Approach	Frequency (MHz/GHz)	Fractional Bandwidth (%)	Electrical Size (ka)	Efficiency (%)	Gain Deviation (dB)	3-D Printed
[1]	Combination of electric and magnetic dipole	2.47 GHz	N/A	0.47	79.2	5.2	No
[2]	Complementary dipole	2.4 GHz	5	N/A	N/A	6.8	No
[10]	Complementary dipoles	2.45 GHz	0.99	0.73	90	3.14	No
[13]	Magnetic dipole	2.45 GHz	4.1	1.23	82	5.7	No
[15]	Patch with ground	2.4 GHz	4.48	0.98	90	1.9	No
[18]	Complementary dipoles	993.5 MHz	0.50	0.33	30	3.8	No
[23]	Crossed dipoles	2.395 GHz	11.27	1.14	N/A	5.8	No
[24]	Four L-shaped Monopoles	2.450 GHz	20.82	1.63	82	5.75	No
[25]	Combination of electric and magnetic dipole	959 MHz	2.4	0.48	81	4.5	Yes
[27]	SSR Based	763 MHz	1.05	0.68	77	2.88	No
[28]	Orthogonal Electric dipoles	895-924 MHz	3.2	N/A	87	6	No
[30]	Monopole AoP	2.4 GHz	11.7	0.4	N/A	6.84	Yes
[36]	Wounded dipole	911.25 MHz	0.77	0.24	N/A	N/A	No
[37]	Magnetic SRR	762 MHz	1.05	0.68	77	3	No
[39]	Angled dipoles	2.451 GHz	6.12	1.28	90	6.4	No
[53]	Loop antenna with truncated ground plane	3.29 GHz	N/A	N/A	42.8	6.2	No

Table 1 shows that a planar quasi-isotropic antenna in its simplest form can be designed by using the complementary dipole approach. Some other approaches such as meandering and metamaterial inspired designs, can be employed to realize quasi-isotropic antenna have also been reported. Nevertheless, these techniques are somewhat more complex than using complementary dipole. Further, the electrical parameters show a trade-off with different design approaches. Overall, bandwidth of compact planar quasi-isotropic antennas is usually very small. Some wide band quasi-isotropic antennas were designed using multiple monopole or dipole techniques that are low cost, support high data rates, and have relatively low power requirements [23], [24], [30].

B. QUASI-ISOTROPIC ANTENNAS USING 3-D PRINTING TECHNOLOGY

The demand for the fabrication of electromagnetic structures using 3-D printing technology has significantly increased during the last few years [7], [25], [30], [31], [38], [54]. This is due to the fact that the 3-D printing technology offers several advantages over traditional fabrication methods, for instance, low cost, ease of fabrication, lightweight, smaller form-factor, and being more bio-friendly. Based on these advantages, several quasi-isotropic antennas have been presented [44]–[47].

A 2.45 GHz additively manufactured, inkjet printed, 3-D in-package antenna was presented for marine animal monitoring purpose [7]. The design consisted of a meandered dipole, which was folded as a split-ring resonator structure that generates orthogonal electric and magnetic dipoles simultaneously, thus generating a quasi-isotropic radiation pattern. A low-cost antenna design with wide bandwidth and isotropic radiation characteristics for both GSM bands consisting of 3-D geometry is very suitable for variety of GSM applications. To design such, an on-package monopole antenna with a near-isotropic radiation pattern with dual-band response is presented [54]. To achieve an isotropic radiation pattern in both bands, their current distributions must satisfy the theoretical condition of a 90° phase difference for both operating frequencies at the same time. Therefore, the dimen-

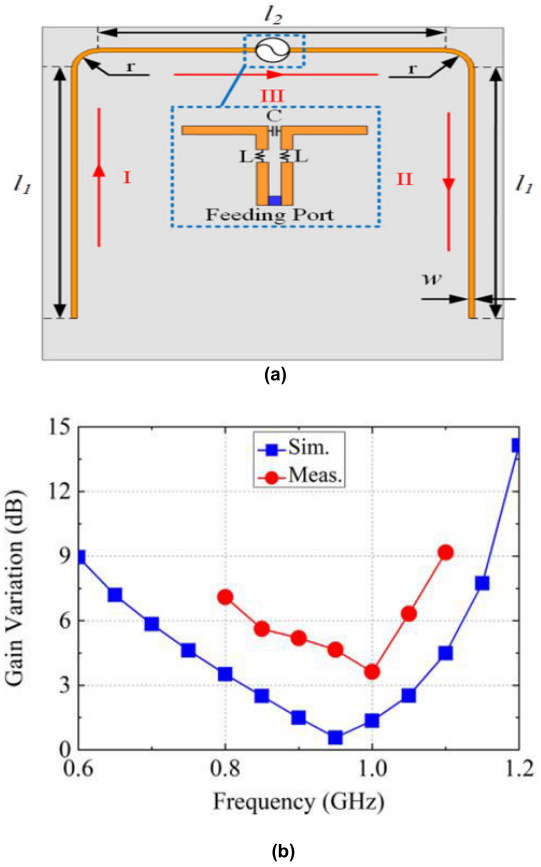

FIGURE 12. Quasi-isotropic antenna in planar configuration, (a) antenna design, (b) axial Ratio [55].

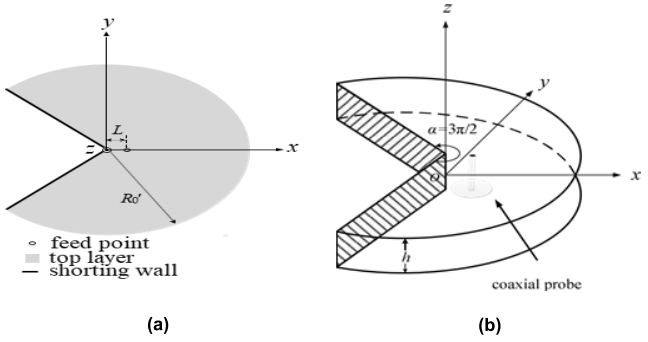

FIGURE 13. Proposed antenna, (a) top view, (b) whole view [13].

sions of the antenna and the box are optimized to have a phase difference of 90° for both bands. The antenna was designed using an additive manufacturing technique and was optimized to work with embedded electronic components and a large black metal battery within the available space. The proposed design and fabricated prototype are shown in Fig. 14. At frequencies of 900 and 1800 MHz, the measured maximum gains were 0.90 and 1.71 dBi, whereas the measured gain variations were 8.92 and 9.99 dB, respectively. An electrically small antenna that operates in the ISM 900 MHz band was proposed in [25]. The antenna achieved a quasi-isotropic

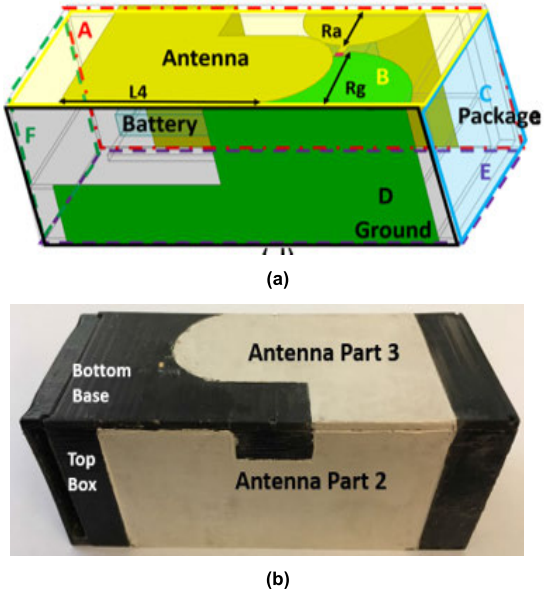

FIGURE 14. (a) Proposed design of the antenna, (b) fabricated prototype [54].

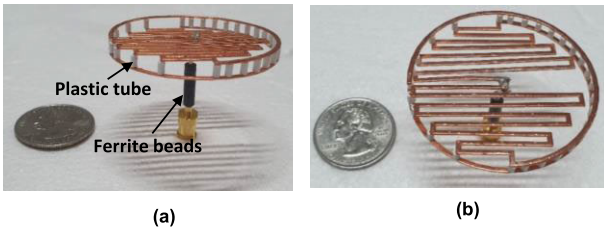

FIGURE 15. Antenna prototype (a) top and bottom structures, (b) perspective view of assembled structure [25].

radiation pattern by integrating small electric and magnetic dipoles. The antenna was fabricated using 3-D printing technology. It consisted of a core meander dipole antenna and a circulating loop antenna, as shown in Fig. 15. The loop antenna can be split into two parts: a clockwise part at the bottom and a counterclockwise part at the top. The current was fed into the center of the meandered electric dipole, generating a coherent current in the loop structure that flows in one direction. The meander line made the antenna self-resonant. The proposed antenna had a radiation efficiency of 81% at 959 MHz, and a 4.5 dB maximum gain deviation. Furthermore, an additively manufactured, 3-D printed on-package, T-shaped monopole antenna with nearly isotropic coverage was presented in [30]. The antenna was designed with an in-package Wi-Fi chip and a battery. A nominal gain of 1.78 dBi and a gain deviation of 6.84 dB were obtained within the 2.4 to 2.7 GHz frequency range.

C. THREE-DIMENSIONAL QUASI-ISOTROPIC ANTENNAS USING OTHER TECHNOLOGIES

One of the advantages of quasi-isotropic antennas is that they can easily be designed in three-dimensional configuration. 3-D antennas are intensively used for on-package applications and miniaturization purposes, as 2-D antennas require a large planar space. These antennas are also

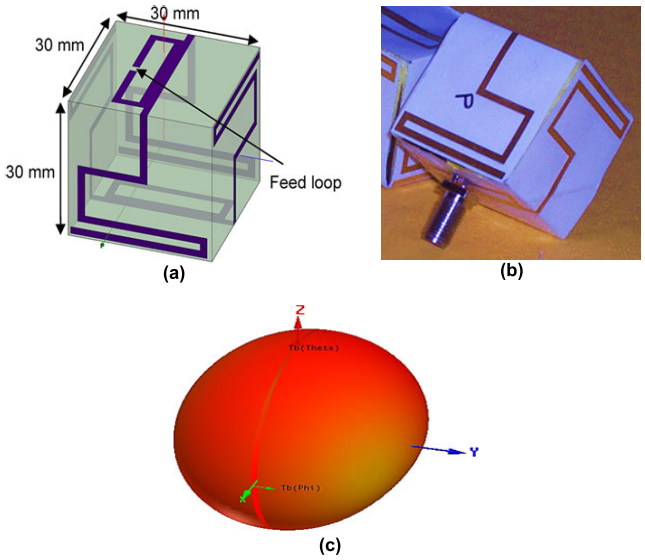

FIGURE 16. 3-D cubic antenna (a) presented antenna, (b) fabricated prototype, (c) radiation pattern [38].

lightweight and easy to mount on surface. Based on these and several other advantages offered by 3-D configuration, various 3-D quasi-isotropic techniques have been reported [25], [30], [31], [38], [54], [60], [61].

In [38], a 3-D cubic quasi-isotropic antenna for wireless sensor networks and RFID applications was presented as shown in Fig. 16. The design contains a meander-line dipole antenna configuration folded into a cubic structure. The quasi-isotropic radiation pattern is achieved by optimizing the arms of the dipole and by the inductive coupling matching technique. This antenna was designed for the UHF RFID 902 MHz–928 MHz frequency band. It is worth mentioning that the designed antenna can easily be integrated with sensor equipment inside the cube, allowing smart and robust packaging. The antenna had an almost isotropic radiation pattern with an efficiency of about 72% and a gain of 0.5 dBi within the spatial coverage. Similarly, a compact shorted patch coaxial fed antenna with a quasi-isotropic radiation pattern was presented in [15]. The design consisted of a quarter-wave rectangular radiating patch at 2.4 GHz, a small ground plane, and a metal sidewall connecting the patch and the ground with an aired substrate between them, as shown in Fig. 17. The antenna operated in its fundamental TEM mode; the electric field generated magnetic current on the surface of the open-ended aperture and the magnetic field generated electric current on the surface of the shorted sidewall.

Due to the inherent phase difference of 90° between electric and magnetic fields, perpendicular electric and magnetic currents were generated on the shorted sidewall and open-ended aperture, respectively, generating a quasi-isotropic radiation pattern without requiring a complex feeding network. A gain deviation of 2 dB was observed over the entire radiating surface of the antenna. Table 2 presents various non-planar quasi-isotropic antennas. Different key performance

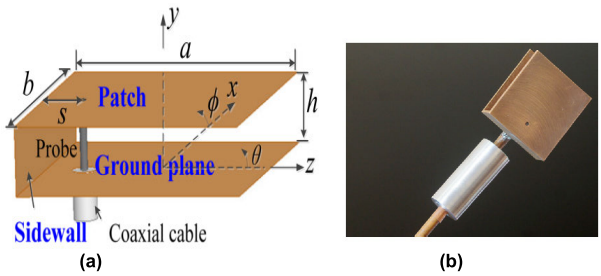

FIGURE 17. Quasi-isotropic shorted patch antenna (a) design, (b) fabricated prototype [15].

parameters, including operating frequencies, fractional bandwidth, electrical size, gain deviation etc., are compared with the respective adopted techniques. Some non-planar techniques offer electrically small designs [7], [17], [25], [41] that are very useful in complex circuitry design environments, where there are space constraints. It is worth mentioning that in contrast to fused deposition modeling (FDM), stereolithography (SLA) 3-D printing technology, due to its better resolution and precision, is most suitable for designing quasi-isotropic antennas. As quasi-isotropic antennas are very sensitive and slight variation in design leads to higher gain deviation, especially for higher frequencies, 3-D printing technology is preferred due to its better resolution and precision. Furthermore, for designing the conductive pattern, we can use inkjet printing in combination with the 3-D printing technology reported in [54]. Nano-polycrystalline copper coating technologies can also be employed when the pattern is a bit complicated and manual cutting of copper tape is challenging. Notably, the radiation efficiency of 3-D printed quasi-isotropic antennas is lower compared to antennas designed using PCB technologies [7], [25], [30], [38]. This is due to the lossy filament used in the 3-D printing fabrication process. However, this lower radiation efficiency does not influence the quasi-isotropic radiation characteristics of 3-D printed antennas. Miniaturized and multiband antennas are inevitable components of modern wireless devices because of their low-cost and space-saving attributes [12], [31], [54], [56], [71], [72].

D. DUAL-BAND QUASI-ISOTROPIC ANTENNAS

In [56], an electrically small dual-band quasi-isotropic antenna was reported. The design consisted of a small dipole with extended arcs wounded in opposite directions etched at the upper and the lower side of the substrate, creating a current distribution similar to a loop antenna, as shown in Fig. 18. The cross electric and magnetic dipole generated a quasi-isotropic pattern, and to achieve a dual-band response, a similar radiating element of different sizes was connected in parallel. The antenna was low profile, with an electrical size of 0.48 ka. The reflection coefficient at the port is illustrated in Fig. 18(b), showing that the antenna resonated at two different frequencies of 900 MHz and 1.75 GHz with gain deviations of 5.83 dB and 8.24 dB, respectively. Radiation

TABLE 2. Summary of non-planar quasi-isotropic antennas with their respective parameters and adopted techniques.

Ref.	Design Approach	Frequency (MHz/GHz)	Fractional Bandwidth (%)	Electrical Size (ka)	Efficiency (%)	Gain Deviation (dB)	3-D Printed
[3]	Complementary dipoles	2.4 GHz	7	N/A	>90	7.9	No
[7]	Meandered folded dipole on 3-D cuboid	2.4 GHz	2.9	0.49	N/A	3.6	Yes
[12]	SSR with folded dipole	868 MHz	5	0.47	76	4	No
[14]	Complementary dipoles	2.44 GHz	6.9	1.05	N/A	5.6	No
[17]	Magnetic Dipoles	888 MHz	1.8	0.41	89	5.6	No
[27]	SSR Based	763 MHz	1.05	0.68	77	2.88	No
[35]	Loop SWA	327.33 MHz	2	0.42	93.2	3	No
[38]	Meandered dipole in a cube	930 MHz	N/A	0.51	72	N/A	Yes
[41]	Multiple dipoles	1.5 GHz	15	0.9	96	N/A	No

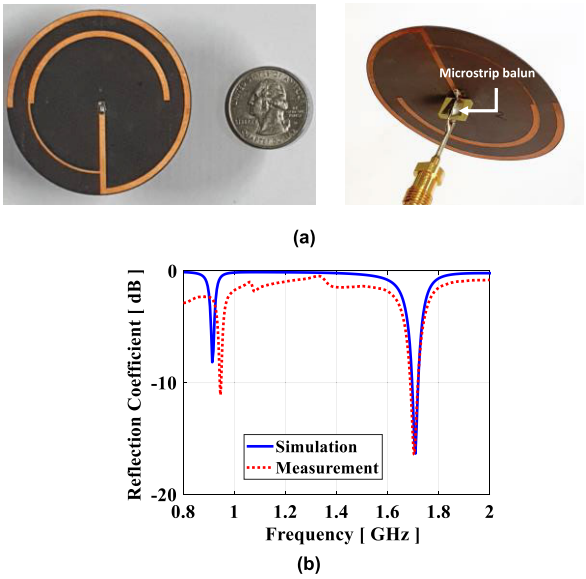

FIGURE 18. Dual-band quasi-isotropic antenna (a) fabricated prototype, (b) reflection coefficient [56].

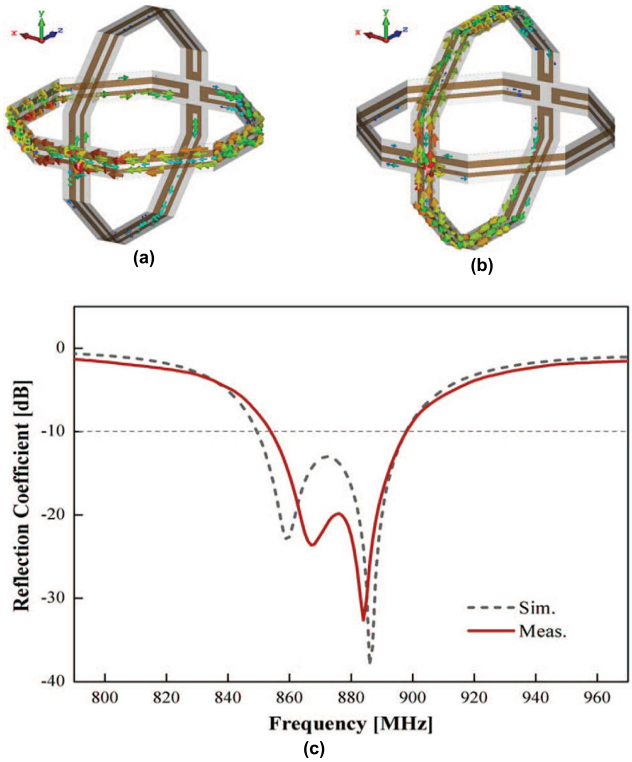

FIGURE 19. Current distribution (a) at first resonance (859 MHz), (b) at second resonance (886 MHz), (c) simulated and measured reflection coefficients [12].

efficiencies of 63% and 91% were observed for lower frequency and higher frequency bands, respectively.

Due to the electrically small configuration, the impedance bandwidth for both bands was very narrow, which is a limitation of this configuration. Hence, integrating such an antenna with the communication system can degrade the performance of the system and detune the resonance. To increase the impedance bandwidth, both resonance frequencies can be merged. For instance in [12], a compact dual-band quasi-isotropic RF energy harvesting antenna was presented, where both bands resonated close to each other to enhance the bandwidth. The proposed design consisted of two perpendicular folded split-ring resonators (FSRR), one in the horizontal

TABLE 3. Summary of dual-band quasi-isotropic antennas with their respective parameters and adopted techniques.

	Design Approach	Frequency (MHz/GHz)	Fractional Bandwidth (%)	Electrical Size (ka)	Efficiency (%)	Gain Deviation (dB)	3-D Printed
[9]	Orthogonal SRR	792 MHz/ 1124 MHz	2.8/ 1.8	0.47	86/ 85.5	4.42/ 5.76	No
[31]	Electric dipoles	900 MHz/ 1800 MHz	8.9/ 34.4	1.16	N/A	8.9/ 9.9	Yes
[54]	Wire monopole	900 MHz/ 1800 MHz	9.3/ 49.1	N/A	N/A	5.3/ 9.5	Yes
[56]	Electric dipole and loop	942 MHz/ 1.71 GHz	N/A	0.49	57/ 95	5.83/ 8.24	No

plane and the other in the vertical plane. This system was fed through via holes connecting the feeding points of two elements. Such arrangement achieved a quasi-isotropic pattern with enhanced bandwidth. The current distributions in Fig. 19 (a) and Fig. 19(b) show that at first resonance, the x-oriented FSRR resonated only acting as an electric dipole in the x-axis and magnetic dipole in the y-axis, which resulted in dual polarization in the xz-plane. On the other hand, at the second frequency, the y-oriented FSRR resonated only acting as an electric dipole in the y-axis and magnetic dipole in the x-axis, resulting in dual-polarization in yz-plane. The electric and magnetic dipoles generated a quasi-isotropic radiation pattern with a gain deviation of 4.0 dB at both resonant frequencies. The reflection coefficient graph illustrates that the antenna resonated at 868 MHz and 884 MHz, with a 10-dB bandwidth of about 5%. Moreover, the radiation efficiency was higher than 76%, and the maximum realized gain was from 0.94 to 1.98 dBi. Although, by using this procedure, one can increase the impedance bandwidth, it will still not be wide enough to cover various desired applications. Therefore, numerous quasi-isotropic antennas with wideband characteristics have been reported, which are presented in the next section. Table 3 summarizes a few key performance parameters of various dual-band quasi-isotropic antennas, including operating frequencies, fractional bandwidth, gain deviation, etc.

It can be noted that the dual band is achieved at the expense of gain deviation and efficiency.

E. WIDEBAND QUASI-ISOTROPIC ANTENNAS

Wideband antennas have sparked a lot of interest in the industry and academia recently due to their low cost, straightforward design, ability to support high data rates, and relatively low power requirements. Modern IoT applications demand connectivity among devices over wide frequency bands and full spatial coverage. To address this, different quasi-isotropic antennas with wideband coverage have been reported in [24], [42], [48], [51], [57], [73]. Note that wideband characteristics can be achieved by merging the resonance of the driven and parasitic element. For instance, the antenna designed in [57] consisted of an elliptical ring and a parasitic arm, as shown in Fig. 20. This system had a vast bandwidth ranging from 820 MHz to 3.5 GHz and was suitable for CDMA, GSM900, GSM1900, 3G, 4G, and Wi-Fi bands. The vertical polarization was achieved by the elliptical ring and horizontal polarization by making a horizontal slot in the antenna. The parasitic arm was added to the antenna to provide a uniform radiation pattern with almost equal horizontal and vertical field components over the entire frequency range. With wideband and uniform radiation patterns, these antennas can find applications in UAVs, RF energy harvesting, and RSSI measurements. Wideband quasi-isotropic antenna can also be designed by four sequentially rotated L-shaped monopoles connected by a compact feeding network of equal magnitude and with sequential phase delay of 90°, as reported in [24].

M1, M2, M3, and M4 are four monopole elements that are excited with different phases to obtain radiation patterns in different directions. The antenna design is shown in Fig. 21, along with the radiation patterns with various different steps. For instance, in step 1, only M1 and M3 are excited with equal amplitude and a phase difference of 180°; the achieved radiation pattern is depicted in Fig. 21 (b). Similarly, in step 2, only M2 and M4 are excited with equal amplitudes and 180° phase difference generating the radiation pattern of Fig. 21 (c). In step 3, M1, M2, M3, and M4 are excited with equal amplitude and phases of 0°, 0°, 180°, and 180°, resulting in the radiation pattern shown in Fig. 21 (d). Similarly, in step 4, M1, M2, M3, and M4 are excited with equal amplitude as well as equal phases, and the obtained radiation pattern is depicted in Fig. 21 (e). Lastly, when M1, M2, M3, and M4 are excited with equal amplitude and phase differences of 0°, 90°, 180°, and 270°, the desired quasi-isotropic radiation pattern can be achieved, as shown in Fig. 21 (f). Figure 21 (g), presents the gain deviation graphs which is less than 6 dB for the entire range. The measured 6.9% wider impedance bandwidth with only a 6-dB gain deviation was much better in the case of quasi-isotropic antennas. It is obvious from all the tables herein that a limited number of quasi-isotropic antennas have been reported with wide impedance bandwidth characteristics in both planar and non-planar configurations.

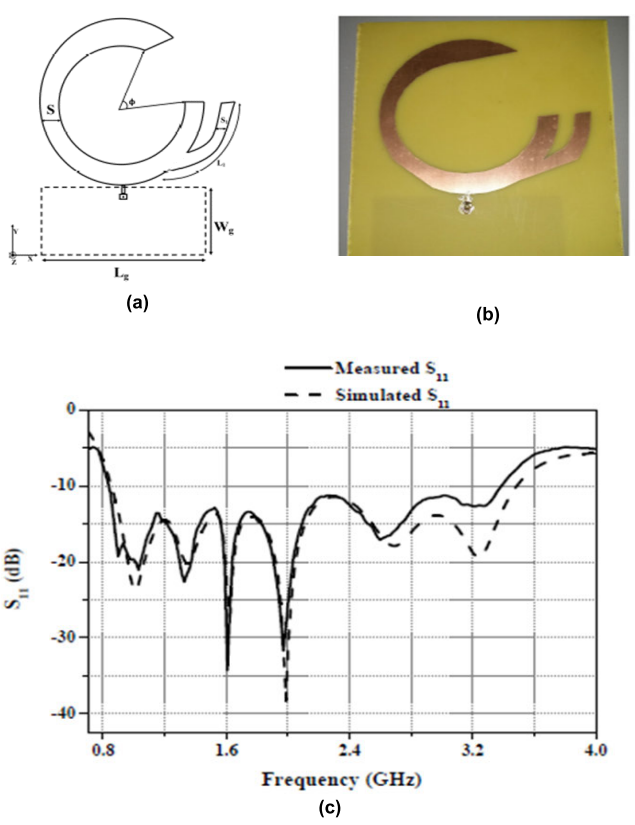

FIGURE 20. Broadband quasi-isotropic antenna (a) modified elliptical ring antenna, (b) fabricated prototype, (c) simulated and measured S_{11} plot [57].

F. CIRCULARLY POLARIZED QUASI-ISOTROPIC ANTENNAS

The attribute inherently exhibited by quasi-isotropic antennas to suppress multipath interference and reception of signals irrespective of the orientation of the transmitting and the receiving antenna can be widely used to design circularly polarized antennas for portable devices [32], [58]–[61].

One of the interesting techniques for designing quasi-isotropic antennas in miniaturized form uses inverted F antennas, as proposed in [28]. Circular polarization can be achieved by arranging four inverted-F antenna elements in a rotational geometry. To optimize the efficiency of the antenna, the top layer of the antenna was designed using a low permittivity substrate, whereas the bottom layer, which held the feeding network, was designed with a high permittivity substrate to reduce size. The antenna resonated at 2.4 GHz, and the efficiency and bandwidth of the antenna were 65% and 100 MHz, respectively. The reduction in efficiency and bandwidth was probably due to the use of a high permittivity substrate. A quasi-isotropic radiation pattern was observed, with an absolute gain deviation of only 3.6 dBi. The antenna showed circular polarization in upward and downward large circular sectors with an average 3 dB axial ratio and a beam width of 105°. In [60], a 3-D on-package antenna was designed by combining three orthogonal dipole antennas and then optimizing using the particle swarm optimization

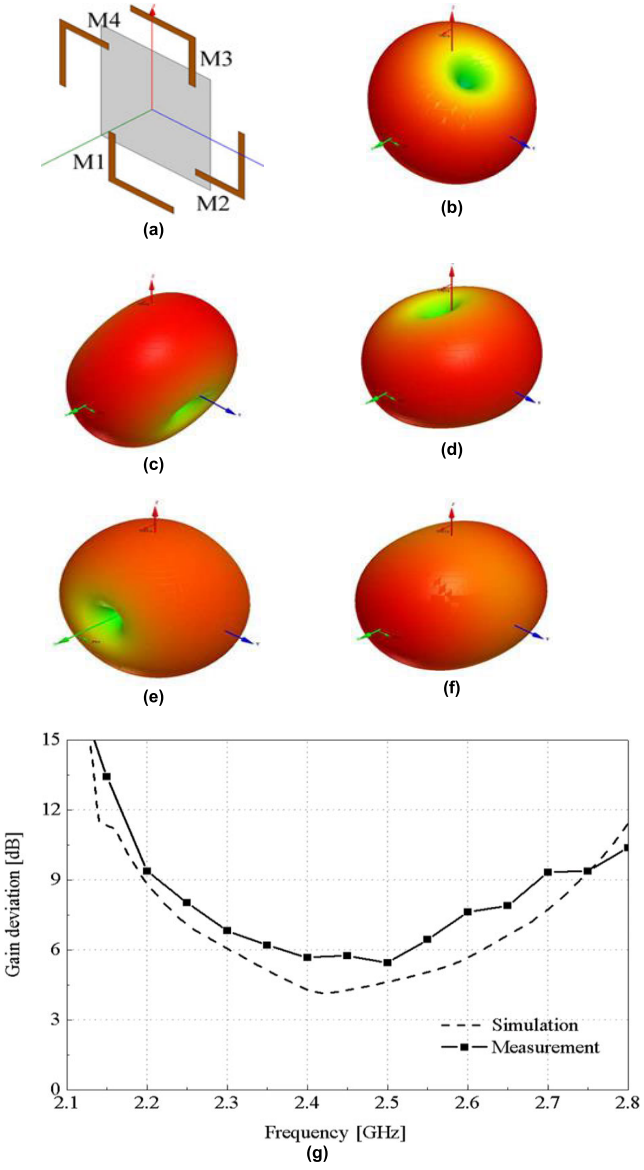

FIGURE 21. (a) Sketch of four L-shaped monopoles; (b) only M1 and M3 are excited with equal amplitude and 180 phase difference; (c) only M2 and M4 are excited with equal amplitudes and 180 phase difference; (d) M1, M2, M3, M4 are excited with equal amplitude and phases differences of 0, 0, 180, 180; (e) M1, M2, M3, M4 are excited with equal amplitude and phases; (f) M1, M2, M3, M4 are excited with equal amplitude and sequential phases of 0, 90, 180, 270. (g) the gain deviation over the broad range [24].

(PSO) technique to achieve circular polarization and near isotropic coverage simultaneously. The three half-wavelength dipoles were mounted on the orthogonal edges of a cubic box, as shown in Fig. 22. PSO algorithm was applied to determine the phase conditions to achieve maximum CP coverage while maintaining the isotropic radiation pattern. A detailed guideline for the design and optimization is provided in [60]. The antenna showed impedance matching from 1.34 GHz to 1.81 GHz.

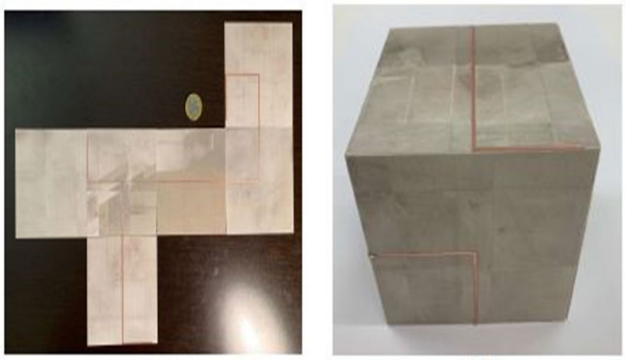

(a) (b)

FIGURE 22. (a) Fabricated roger boards with metallic patterns for three half wave dipoles, (b) antenna in cubic form [60].

Due to the orthogonal arrangement of dipoles, the antenna showed isotropy of almost 93% and CP coverage of ∼18% at 1.52 GHz.

Table 4 presents different performance parameters of wideband and circularly polarized antennas including operating frequency, fractional bandwidth, radiation efficiency and gain deviation. The gain deviation and fractional bandwidth varies with the design approaches.

In single band quasi-isotropic antennas, the highest achieved bandwidth is 11.7% with a gain deviation of 6.84 dB [30]. For the dual band antennas, the highest achieved bandwidth is 8.89 and 34% with the gain deviation of 8.9 dB and 9.9 dB, respectively [31]. For the wideband antennas, the highest achieved bandwidth is 20.82% with the gain deviation of around 6 dB [24]. So far, as the circularly polarized quasi-isotropic antennas are concerned, the highest achieved bandwidth is 4.1%. However, other relevant information such as gain deviation and axial ratio bandwidth have not been reported [52], [59]–[62].

In some studies, quasi-isotropic antennas are designed to improve the CP coverage over the entire radiating sphere of the antenna [32], [60]. Therefore, it needs further attention and research to explore the wideband and circularly polarized quasi-isotropic antennas.

G. ELECTRICALLY SMALL QUASI-ISOTROPIC ANTENNAS

The miniaturization of the sub-systems of modern wireless devices increases the demand for electrically small antennas. These electrically small antennas are very useful in complex circuitry design environments, where there are space constraints [74], [75]. The placement, orientation, and relative position of the antenna in such devices is typically random and unknown. Thus, the quasi-isotropic antennas are preferred in such complex environments. Several electrically small quasi-isotropic antennas have been proposed [1], [10], [56], [62], [63], [13], [18], [25], [27], [35]–[37], [39]. It is believed that the SSR structure generates electric and magnetic dipoles with equal magnitude and orthogonal radiation pattern. To demonstrate this, an electrically small unipolar antenna with quasi-isotropic characteristics was presented in [61].

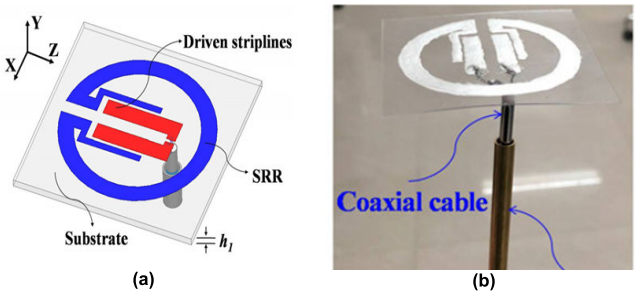

(a) (b)

FIGURE 23. Split-ring resonator based electrically small quasi-isotropic antenna (a) 3-D model, (b) fabricated prototype [27].

This antenna was designed on a 150-μm thick PDMS substrate. The patch consisted of a split-ring resonator with the stripes stretched inside and a pair of driven strip lines that extend inward from the end of the ring gap to its center. The antenna was fed directly by a coaxial cable linking the two ends of the strip lines, as shown in Fig. 23. Since the antenna was electrically small, fractional bandwidth is minimal, around 1.05%, and efficiency was higher than 75%. The proposed antenna had an overall gain deviation of 2.88 dB, which is, in principle, lower than the minimum value of 3 dB.

H. METAMATERIAL-BASED QUASI-ISOTROPIC ANTENNAS

Metamaterials are artificial media that represent the unusual behavior of electromagnetic waves. Metamaterials can be employed in different types of antenna designs [62], [73], [76]–[79]. The quasi-isotopic designs have also been reported using metamaterials as split-ring resonators (SRR) [9], [17], [37], through thin Kapton film [26], realizing E-field-driven *LC* metamaterials resonator, and by employing multiple metamaterial unit cells [11]. The metamaterial technique can be categorized mainly under the approach of orthogonality [17], [37]. However, some quasi-isotropic antennas have been designed using two or more monopoles, or electric and magnetic dipoles as well [9], [26].

In [26], an isotropic antenna was demonstrated on a flexible substrate using a thin folded dipole and split ring resonator to achieve quasi-isotropic coverage, as depicted in Fig. 24. The SRRs were excited by gap coupling to the dipole, and by changing the radius of the flexible film, the resonance frequency shifted accordingly. When the radius of the curved film was decreased by rolling it, the frequency increased and vice-versa. The antenna possessed an electrical size (ka) of 0.75, with a maximum gain of 1.83dBi and a maximum efficiency of 83%. The antenna was made of a cylindrical dielectric resonator with a small ground plane, as shown in Fig. 24, where the ground plane and DR plane work as electric and magnetic dipoles, respectively. By the interaction of both orthogonal dipoles, a quasi-isotropic radiation pattern can be attained.

TABLE 4. Summary of wideband/circularly polarized quasi-isotropic antennas with their respective parameters and adopted techniques.

Ref.	Design Approach	Frequency (MHz/GHz)	Fractional Bandwidth (%)	Circularly Polarization Coverage	Efficiency (%)	Gain Deviation (dB)	3-D Printed
[22]	Inverted-F antenna	10.5 GHz	15	N/A	N/A	10.78	No
[24]	Multiple monopoles	2.45 GHz	20.82	N/A	80	6	No
[31]	Electric Dipole	900 / 1800 MHz	9.8 / 34	N/A	N/A	8.9 / 9.9	Yes
[32]	Multiple dipoles	2.4 GHz	4.1	Yes	>65	3.6	No
[48]	Meander dipole	840-950 MHz	20	N/A	N/A	N/A	No
[51]	Multiple dipoles	880-940 MHz	8.5	N/A	90	<6	No
[60]	Orthogonal Dipoles	1.52 GHz	30	Yes	N/A	N/A	Yes

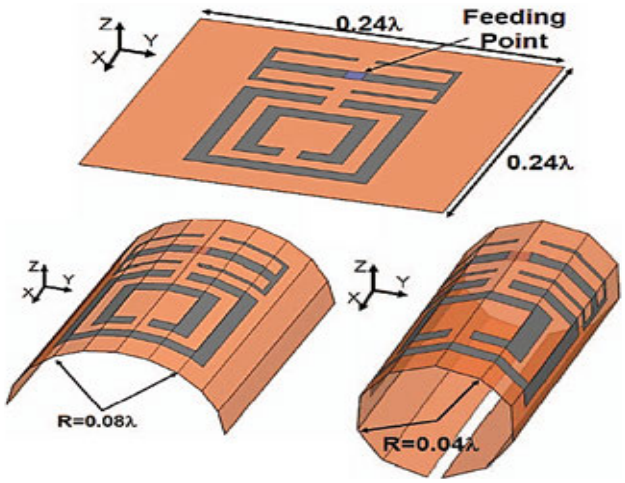

FIGURE 24. An example of a flexible metamaterial-based isotropic antenna where SRR is designed on a Kapton substrate [26].

I. DIELECTRIC RESONATOR-BASED QUASI-ISOTROPIC ANTENNAS

Based on attributes such as ease of excitation, low loss, lightweight, and relatively wide impedance bandwidth, dielectric resonator antennas (DRA) are extensively used in wireless communication systems [3], [14].

A compact microstrip-coupled slot-fed quasi-isotropic DRA with a filtering response was designed [3] and depicted in Fig. 25. The ground plane and microstrip feedline was inverted to integrate filtering response. The antenna showed impedance bandwidth ranging from 2.31 to 2.48 GHz, generating two radiation nulls beside the passband that helped in achieving high-frequency selectivity. An average minimal gain deviation of 5.8 dB in the full space of 360° was observed.

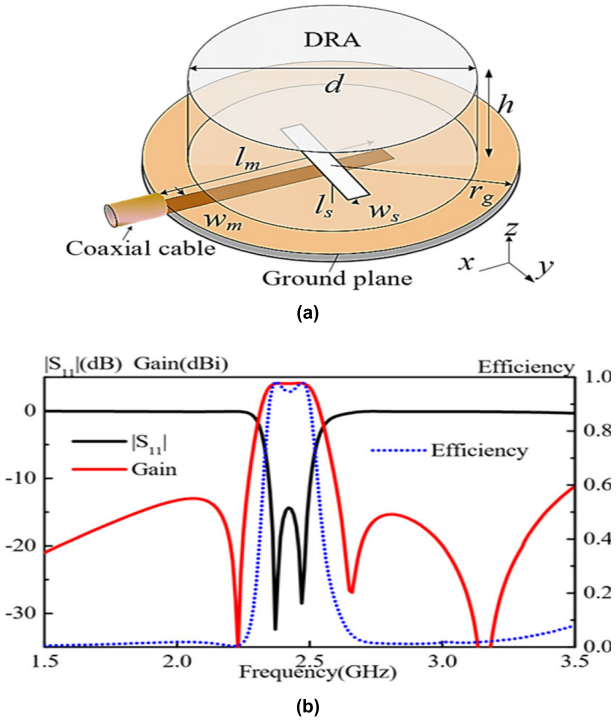

FIGURE 25. Dielectric resonator based quasi-isotropic antenna (a) proposed DRA design, (b) simulated gain, reflection coefficient, and efficiency graph [14].

Similarly, in another study [14], a coaxial probe-fed quasi-isotropic DRA with a compact ground plane for a 2.4 GHz WLAN was presented. The ground plane and the fundamental mode of the rectangular DR served as electric and magnetic dipole, respectively. The combination of both magnetic and electric dipoles generated a quasi-isotropic radiation pattern. The antenna can be tuned by altering the length and position

of the feed. The proposed antenna had a quasi-isotropic radiation pattern with a gain variation of 5.6 dB over the entire spherical region. Gain deviation can be further reduced by using a narrow ground plane.

IV. PERFORMANCE VERIFICATION AND APPLICATIONS PERSPECTIVES OF QUASI-ISOTROPIC ANTENNAS

A. PERFORMANCE VERIFICATION

Due to the arbitrary distribution of indoor wireless signals, the incoming signal direction to the receiver is generally random. In such a scenario, an antenna with a quasi-isotropic pattern having nearly full spatial coverage can be more suitable for receiving signals compared to a conventional omnidirectional antenna. The antenna designed in [1] was evaluated for link reliability of wireless links for the indoor environment case using the packet delivery ratio (PDR) and received signal strength indicator (RSSI) values at 2.47 GHz. The performance of the presented antenna was compared with the transmitter and receiver pair of omnidirectional antennae as a reference under different circumstances, with transmitted power of 5 dBm, and receiver possessed sensitivity of −95 dBm. The PDR and RSSI graphs for the measured values are shown in Fig. 26. For the line of sight (LOS) communication, there was a minimal difference between the two pairs. However, a quasi-isotropic antenna performance was slightly better because of the addition of scattering fields from different obstacles. In the case of non-line of sight (NLOS) communication, the use of an omnidirectional antenna degraded PDR and RSSI due to metal obstacles and weak multipath signals, whereas a quasi-isotropic antenna provided robust performance in terms of PDR and RSSI for various NLOS positions. PDR and RSSI were also evaluated for the deployment scenario of transmitter and receiver on different floors of the same building. The transmitter was installed on the lower floor, and the vertical separation between the two nodes was around 3.7 m. When the transmitted power was greater than –9 dBm, the proposed design provided approximately 3 dBm gain in terms of RSSI compared to the omnidirectional antenna pair, as depicted in Fig. 26. It also showed PDR greater than 70 for a transmit power level between −11 and −9 dBm, whereas the omnidirectional antenna pair PDR level was less than 35%. In another study [65], a practical demonstration was presented for wireless power reception using the dual band quasi-isotropic antenna. The antenna performance was analyzed under different LOS and NLOS situations using a transmitted power of 15 dBm for all situations and then compared with a reference omnidirectional antenna.

The measured results for the received power signal in Fig. 27 depict that the received power was almost the same for both antennas in the LOS environment. However, due to multipath channels, the peak gain of the quasi-isotropic antenna was higher than that of the reference omnidirectional antenna, while for NLOS positions, the quasi-isotropic antenna usually received more power compared to the omnidirectional antenna because of its uniformity of field intensity. Sensors intended for monitoring purposes in different scenarios, such as drone and UAV's operations, marine animal tagging, and flood monitoring, need to be equipped with antennas that can radiate in all directions so that a stable communication link exists between the transmitter and receiver regardless of their orientation. Quasi-isotropic antennas can

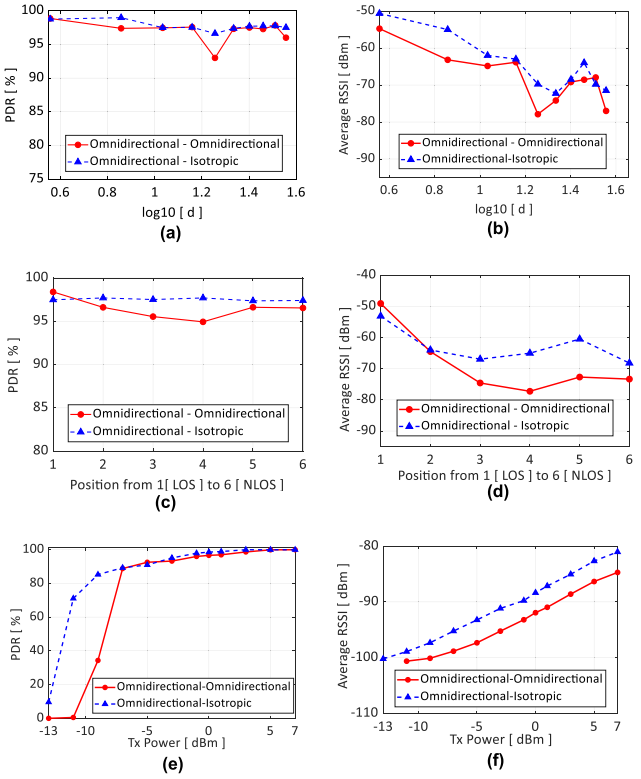

FIGURE 26. Performance verification of quasi-isotropic antenna. (a) PDR for LOS case, (b) RSSI for LOS situation, (c) PDR for NLOS scenario, (d) RSSI for NLOS scenario (e) measured PDR & (f) RSSI for NLOS at different floors of the building [1].

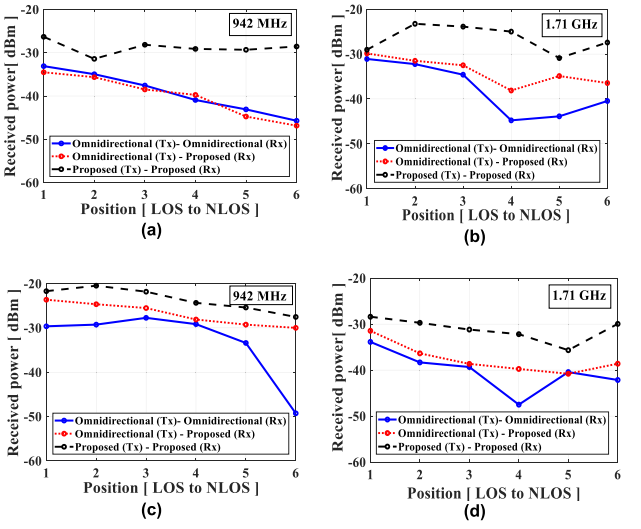

FIGURE 27. Measured received power levels at (a) 942 MHz, (b) 1.71 GHz, (c) 942 MHz, (d) 1.71 GHz [56].

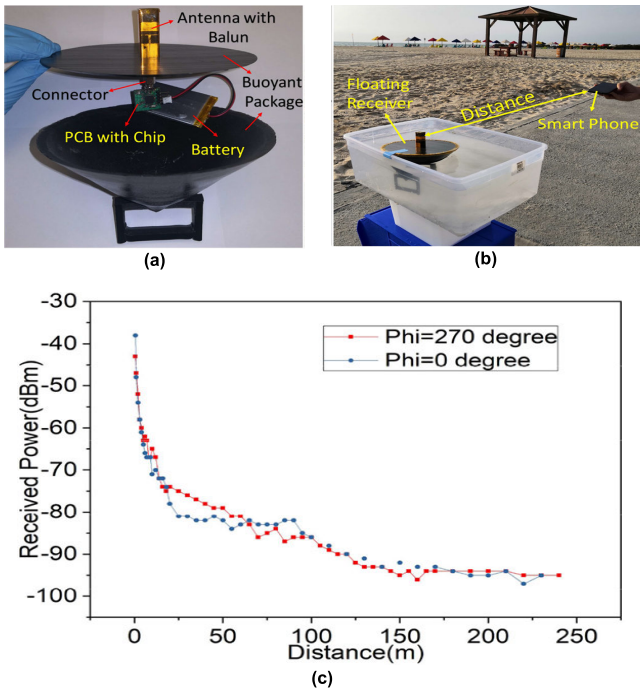

FIGURE 28. (a) Proposed receiver system, (b) active test setup, (c) active range test results [7].

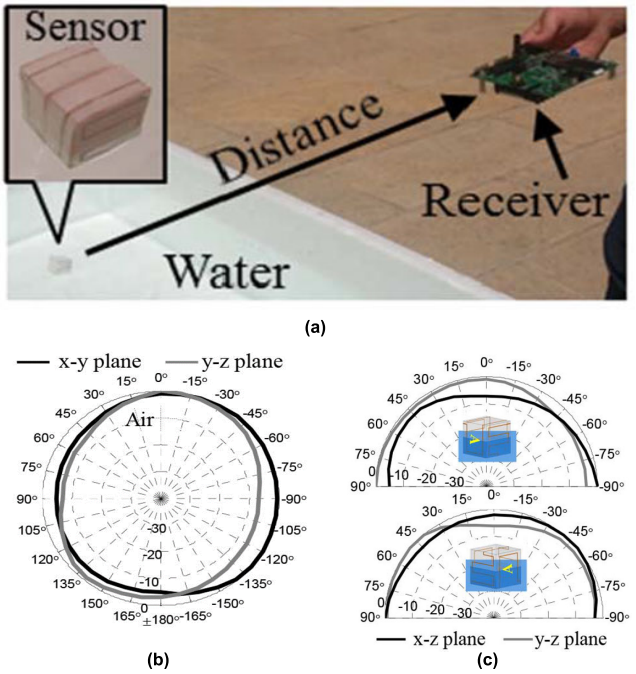

FIGURE 29. (a) Setup for field tests in water, (b) radiation pattern in air, (c) radiation pattern of antenna half immersed in water in two different orientations [64].

play a vital role in such situations [7], [63], [64]. In [7], an on-package antenna was designed for marine animal monitoring purpose. Active and passive tests were conducted to verify the performance of the antenna. During the active test, the antenna was placed in water in an open area to avoid reflection, and a smartphone with a custom-built Bluetooth app was used to measure the received power from the floating antenna. Fig. 28, shows the test setup and the relationship between received power and distance. The maximum gain was obtained at $\phi = 270°$ (or 90°) and minimum gain at $\phi = 0°$ or $(-180°)$, which indicates that at other angles, the communication range will be in between the values at $\phi = 270°$ (or 90°) and $\phi = 0°$ (or $-180°$).

The antenna had a maximum gain deviation of 3.5 dB and a communication link can be established from any direction. In [64], a dipole antenna was implanted on the outer faces of an inkjet-printed buoyant 3-D Lagrangian sensor designed for real-time flood monitoring purpose. The arrangement is shown in Fig. 29 (a). The performance of the prototype was evaluated using field tests in air and in water. The radiated power of the antenna was measured with a transceiver having a sensitivity of half of the sensor was immersed in water, and measurements were conducted from above the water surface. -100 dBm in two different planes in stationary and floating conditions.

Fig. 29 (c) indicates the upper half of the radiation pattern only. The results indicate that the variation in radiation power in different orientations did not exceed -7 dB in all directions, both in air and in water. Hence, the proposed antenna exhibited almost isotropic radiation characteristics.

B. APPLICATION PERSPECTIVES

Due to full spatial coverage, quasi-isotopic antennas are promising candidates for several applications, as shown in Fig. 30. Some applications are discussed in detail in the following section to understand the advantages of using quasi-isotropic antennas.

C. INTERNET OF THINGS

The Internet of Things (IoT) will take connectivity one step further in the near future, as billions of smart devices will communicate with each other to perform various tasks. Most of these devices use Wi-Fi to connect, as it is widely available indoors. Devices intended for use in IoT applications must be able to maintain stable and reliable communication links, regardless of their orientation, as these devices can be dispersed in arbitrary positions. Such devices, however, have quite challenging antenna design requirements. To meet these requirements, antenna designers must meet a variety of performance metrics. The intended antenna should be low cost, be able to integrate with miniaturized devices, and radiate equally in all directions to communicate with other devices without being affected by their orientation. Certain antenna designs with quasi-isotropic radiation patterns have been discussed that can be easily integrated with IoT devices [30], [60], [80].

D. RADIO FREQUENCY IDENTIFICATION

Radio frequency identification (RFID) is used in a variety of applications, such as identification, tracking, automatic data

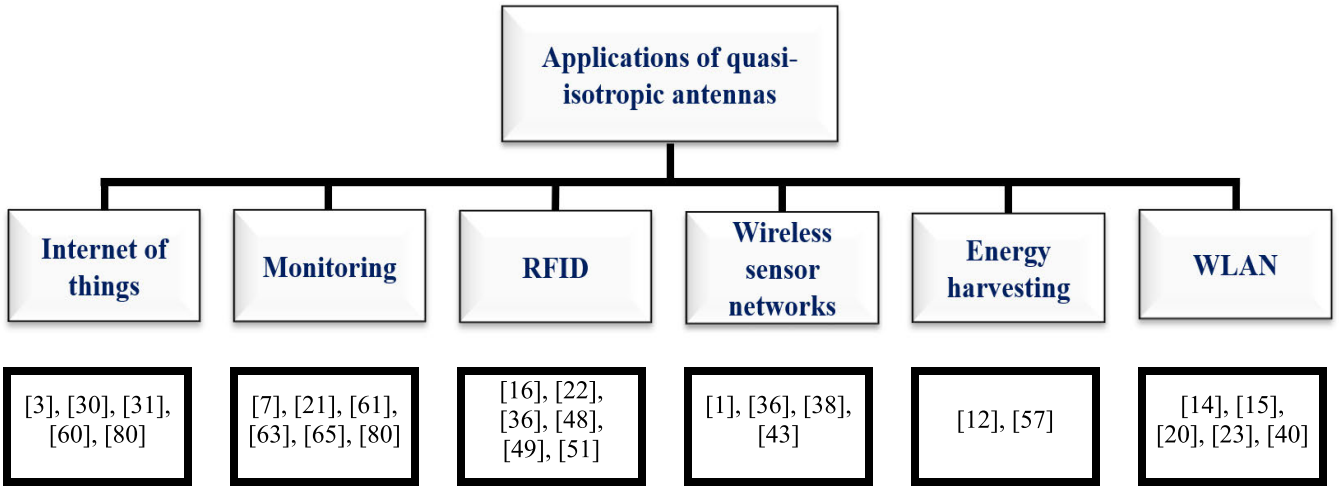

FIGURE 30. Applications of quasi-isotropic antennas.

acquisition, and access control. RFID systems rely heavily on the antennas that are attached to the tags, as its performance significantly affects reading range and error rate. A dipole-type antenna with omnidirectional radiation is the most common RFID tag antenna used in commercial RFID tags. However, they have nulls or very low gains in some directions, resulting in very small reading ranges. To ensure the reliability of the RFID system, the tag should therefore have uniform radiation characteristics in all directions close to isotropic. In this regard, the use of a quasi-isotropic antenna can be handy [16], [22], [36], [48], [49], [51].

E. RF ENERGY HARVESTING

Radio frequency energy harvesting has gained popularity as a battery-free energy source for sensor nodes in wireless communication systems. Recently, the research into zero-power solutions for the Internet of Everything has grown exponentially. Different scavenging techniques, such as mechanical, solar, thermal, and radiofrequency (RF), are being employed to attain battery less solutions. Antenna is the key component in RF energy harvesting. Despite its popularity, dipole antennas are not very efficient owing to polarization mismatches and radiation nulls along their axis direction. Since the radio frequency energy is distributed randomly, receiving antennas with isotropic radiation patterns, which can provide comprehensive coverage of the surrounding space, can be efficient way to harvest ambient energy [12].

V. CHALLENGES AND FUTURE DIRECTIONS

The sensitivity of the radiation characteristics is one of the main challenges in designing quasi-isotropic antennas since a slight design variation can have a significant effect on the gain deviation. For instance, in [63], the gain deviation increased to 12.9 dB from 5.2 dB of computed expectations due to a minor fabrication error that occurs when the top-loaded monopole was combined with the slotted loop configuration. This problem arises whenever there is an air gap within the layers of the antenna design, which is challenging to fabricate with high accuracy as reported in [25]. To overcome this challenge, antenna designs should be chosen in a manner that ensures fabrication with a minimal fabrication tolerance. The next point of concern relates to 3-D printed quasi-isotropic antenna structures especially where 3-D printing filament is not fully covered by conductor pattern. In this case, the radiation efficiency could be lower compared to antennas designed on PCB [7], [7], [25], [30], [38]. This is due to the lossy filaments used in the 3-D printing fabrication process. Even though this lower radiation efficiency of 3-D printed antennas might have not have much influence on the gain deviation, it affects the radiation efficiency so is overall radiation performance of the antenna. On the other hand, the 3-DP quasi-isotropic antenna composed of meandered geometries where the 3-D printed filament is fully covered by metals, the lossy filaments do not have much impact on the radiation characteristics of the antenna.

Multi-band, electrically small isotropic antenna designs also have some notable limitations which need further attention. For instance, the large frequency span between the multiple resonances is hard to achieve as they are strongly related to the size of each resonator. Similarly, as multiple resonators need to be placed, it is usually challenging to design the multi-band isotropic antenna small. Furthermore, it can be noted that multi-band and wideband characteristics is achieved at the expense of gain deviation and efficiency [2], [22], [31], [56]. Therefore, further research is worth to be carried out to design multi-band and wideband quasi-isotropic antennas with minimum gain deviation. Sometimes, the gain deviation of the electrically small quasi-isotropic antennas can be increased due to the current flowing over the outer conductor of the cable, which can effect on the radiation performance during the measurement [56]. As far as polarization purity is concerned, it is rather difficult to achieve uniform polarization in quasi-isotropic antennas since linear polarization cannot span the entire sphere in the antenna

configurations intended to achieve the quasi-isotropic pattern. In other words, polarization varies from linear to circularly polarized by the observation point of the radiation spheres [1]. Therefore, it can be stated that the polarization dependency of the quasi-isotropic antennas in radiation sphere is the practical bottleneck that should be overcome and worth further research.

VI. CONCLUSION

In this work, different design techniques, working principles, and characteristics of various kinds of quasi-isotropic antennas were discussed. We also presented a detailed review and analysis for each study. We believe that this work will provide a guideline for antenna engineers and researchers to build a quasi-isotropic antenna with desirable performance. The reviewed design techniques can be classified into three major categories: orthogonal complementary dipoles, the array of discrete elements mounted on a cylindrical surface, and the method of using multiple monopoles or dipoles. Since the orientation, placement, and relative position of the antenna in small communication devices is usually random and unknown, a quasi-isotropic antenna having near-uniform power distribution in all directions is the most suitable option in such complex environments. Moreover, quasi-isotropic antennas can be very useful for 5G communication technology, RFID systems, RF energy harvesting, IoT, on-body, wearable solutions, wireless access points, drone communications, flood monitoring systems, marine animal monitoring systems, and many more. We believe that the emerging 5G, subsequent systems and subsystems may be equipped with the available and new quasi-isotropic antenna designs targeting multiple bands, higher efficiency, low profile, small gain deviations over spherical coverage, and wider beam width, enabling a robust, fast, and secure communication system.

REFERENCES

[1] S. M. Radha, M. Jung, P. Park, and I.-J. Yoon, "Design of an electrically small, planar quasi-isotropic antenna for enhancement of wireless link reliability under NLOS channels," *Appl. Sci.*, vol. 10, no. 18, p. 6204, Sep. 2020.

[2] J. Kim, J. Park, A. A. Omar, and W. Hong, "A symmetrically stacked planar antenna concept exhibiting quasi-isotropic radiation coverage," *IEEE Antennas Wireless Propag. Lett.*, vol. 19, no. 8, pp. 1390–1394, Aug. 2020, doi: 10.1109/LAWP.2020.3003011.

[3] P. F. Hu, Y. M. Pan, X. Y. Zhang, and B. J. Hu, "A compact quasi-isotropic dielectric resonator antenna with filtering response," *IEEE Trans. Antennas Propag.*, vol. 67, no. 2, pp. 1294–1299, Feb. 2019.

[4] W. Scott and K. Hoo, "A theorem on the polarization of null-free antennas," *IEEE Trans. Antennas Propag.*, vol. AP-14, no. 5, pp. 587–590, Sep. 1966.

[5] V. Bhatnagar and P. Owende, "Energy harvesting for assistive and mobile applications," *Energy Sci. Eng.*, vol. 3, no. 3, pp. 153–173, May 2015, doi: 10.1002/ese3.63.

[6] R. Ganesan, X. M. Raajini, A. Nayyar, P. Sanjeevikumar, E. Hossain, and A. H. Ertas, "BOLD: Bio-inspired optimized leader election for multiple drones," *Sensors*, vol. 20, no. 11, p. 3134, Jun. 2020, doi: 10.3390/s20113134.

[7] H. Liao, Q. Zhang, M. A. Karimi, Y.-H. Kuo, N. Mishra, and A. Shamim, "An additively manufactured 3-D antenna-in-package with quasi-isotropic radiation for marine animals monitoring system," *IEEE Antennas Wireless Propag. Lett.*, vol. 18, no. 11, pp. 2384–2388, Nov. 2019.

[8] C. Deng, Y. Li, Z. Zhang, and Z. Feng, "Design of a three-dimensional folded slot antenna with quasi-isotropic radiation pattern," in *Proc. IEEE Int. Symp. Antennas Propag. USNC/URSI Nat. Radio Sci. Meeting*, Jul. 2015, pp. 588–589, doi: 10.1109/APS.2015.7304680.

[9] J. H. Kim and S. Nam, "Design of a compact dualband quasi-isotropic antenna," *Electron. Lett.*, vol. 53, no. 8, pp. 515–516, Apr. 2017, doi: 10.1049/el.2017.0603.

[10] J. Ouyang, Y. M. Pan, S. Y. Zheng, and P. F. Hu, "An electrically small planar quasi-isotropic antenna," *IEEE Antennas Wireless Propag. Lett.*, vol. 17, no. 2, pp. 303–306, Feb. 2018, doi: 10.1109/LAWP.2017.2787720.

[11] E. S. Pires, G. Fontgalland, M. A. B. Melo, R. R. M. Valle, and S. E. Barbin, "Metamaterial-inspired wire antennas," *IEEE Trans. Magn.*, vol. 49, no. 5, pp. 1893–1896, May 2013, doi: 10.1109/TMAG.2013.2245640.

[12] J.-H. Kim, H. Kim, and S. Nam, "Design of a compact quasi-isotropic antenna for RF energy harvesting," in *Proc. IEEE Wireless Power Transf. Conf. (WPTC)*, May 2017, pp. 1–3, doi: 10.1109/WPT.2017.7953844.

[13] Q. Li, W.-J. Lu, S.-G. Wang, and L. Zhu, "Planar quasi-isotropic magnetic dipole antenna using fractional-order circular sector cavity resonant mode," *IEEE Access*, vol. 5, pp. 8515–8525, 2017.

[14] Y.-M. Pan, K. W. Leung, and K. Lu, "Compact quasi-isotropic dielectric resonator antenna with small ground plane," *IEEE Trans. Antennas Propag.*, vol. 62, no. 2, pp. 577–585, Nov. 2013.

[15] Y. Pan and S. Zheng, "A compact quasi-isotropic shorted patch antenna," *IEEE Access*, vol. 5, pp. 2771–2778, 2017.

[16] L. Liang and S. V. Hum, "A low-profile antenna with quasi-isotropic pattern for UHF RFID applications," *IEEE Antennas Wireless Propag. Lett.*, vol. 12, pp. 210–213, 2013.

[17] J.-H. Kim and S. Nam, "A compact quasi-isotropic antenna based on folded split-ring resonators," *IEEE Antennas Wireless Propag. Lett.*, vol. 16, pp. 294–297, 2017.

[18] X. Xu, H.-C. Huang, and Y. E. Wang, "Isotropic radiation from an electrically small loop-loaded printed dipole," in *Proc. IEEE Int. Workshop Antenna Technol.*, Mar. 2009, pp. 1–4.

[19] Z. Zhang, X. Gao, W. Chen, Z. Feng, and M. F. Iskander, "Study of conformal switchable antenna system on cylindrical surface for isotropic coverage," *IEEE Trans. Antennas Propag.*, vol. 59, no. 3, pp. 776–783, Mar. 2011.

[20] X. Gao, H. Zhong, Z. Zhang, Z. Feng, and M. F. Iskander, "Low-profile planar tripolarization antenna for WLAN communications," *IEEE Antennas Wireless Propag. Lett.*, vol. 9, pp. 83–86, 2010.

[21] H. Gazzah, "Optimum antenna arrays for isotropic direction finding," *IEEE Trans. Aerosp. Electron. Syst.*, vol. 47, no. 2, pp. 1482–1489, Apr. 2011.

[22] L. Pazin, A. Dyskin, and Y. Leviatan, "Quasi-isotropic X-band inverted-F antenna for active RFID tags," *IEEE Antennas Wireless Propag. Lett.*, vol. 8, pp. 27–29, 2009.

[23] G. Pan, Y. Li, Z. Zhang, and Z. Feng, "Isotropic radiation from a compact planar antenna using two crossed dipoles," *IEEE Antennas Wireless Propag. Lett.*, vol. 11, pp. 1338–1341, 2012.

[24] C. Deng, Y. Li, Z. Zhang, and Z. Feng, "A wideband isotropic radiated planar antenna using sequential rotated L-shaped monopoles," *IEEE Trans. Antennas Propag.*, vol. 62, no. 3, pp. 1461–1464, Mar. 2014.

[25] S. M. Radha, G. Shin, P. Park, and I.-J. Yoon, "Realization of electrically small, low-profile quasi-isotropic antenna using 3D printing technology," *IEEE Access*, vol. 8, pp. 27067–27073, 2020, doi: 10.1109/ACCESS.2020.2971316.

[26] I. Kwang Kim and V. V. Varadan, "Flexible isotropic antenna using a split ring resonator on a thin film substrate," in *Proc. IEEE Int. Symp. Antennas Propag. (APSURSI)*, Jul. 2011, pp. 3333–3335, doi: 10.1109/APS.2011.6058698.

[27] Y. Wang, M.-C. Tang, D. Li, K.-Z. Hu, M. Li, and X. Tan, "Low cost, electrically small, quasi-isotropic antenna based on split ring resonator," in *Proc. Int. Appl. Comput. Electromagn. Soc. Symp.-China (ACES)*, Aug. 2019, pp. 1–2, doi: 10.23919/ACES48530.2019.9060708.

[28] C. Cho, H. Choo, and I. Park, "Printed symmetric inverted-F antenna with a quasi-isotropic radiation pattern," *Microw. Opt. Technol. Lett.*, vol. 50, no. 4, pp. 927–930, 2008, doi: 10.1002/mop.23247.

[29] D. Bugnolo, "A quasi-Isotropic' antenna in the microwave spectrum," *IRE Trans. Antennas Propag.*, vol. 10, no. 4, pp. 377–383, Jul. 1962.

[30] Z. Su, K. Klionovski, R. M. Bilal, and A. Shamim, "3D printed antenna-on-package with near-isotropic radiation pattern for IoT (WiFi based) applications," in *Proc. IEEE Int. Symp. Antennas Propag. USNC/URSI Nat. Radio Sci. Meeting*, Jul. 2018, pp. 1431–1432, doi: 10.1109/APUSNCURSINRSM.2018.8608789.

[31] Z. Su, K. Klionovski, R. M. Bilal, and A. Shamim, "A dual band additively manufactured 3-D antenna on package with near-isotropic radiation pattern," *IEEE Trans. Antennas Propag.*, vol. 66, no. 7, pp. 3295–3305, Jul. 2018.

[32] M. Huchard, C. Delaveaud, and S. Tedjini, "Miniature antenna for circularly polarized quasi isotropic coverage," in *Proc. 2nd Eur. Conf. Antennas Propag. (EuCAP)*, 2007, p. 22, doi: 10.1049/ic.2007.0953.

[33] S. Long, "A combination of monopole and slot antennas for isotropic coverage," in *Proc. Soc. Int. Symp. Antennas Propag.*, vol. 12, Jun. 1974, pp. 68–71.

[34] S. A. Long, "A combination of linear and slot antennas for quasi-isotropic coverage," *IEEE Trans. Antennas Propag.*, vol. AP-23, no. 4, pp. 572–576, Jul. 1975.

[35] A. Mehdipour, H. Aliakbarian, and J. Rashed-Mohassel, "A novel electrically small spherical wire antenna with almost isotropic radiation pattern," *IEEE Antennas Wireless Propag. Lett.*, vol. 7, pp. 396–399, 2008.

[36] H.-K. Ryu, G. Jung, D.-K. Ju, S. Lim, and J.-M. Woo, "An electrically small spherical UHF RFID tag antenna with quasi-isotropic patterns for wireless sensor networks," *IEEE Antennas Wireless Propag. Lett.*, vol. 9, pp. 60–62, 2010.

[37] Y. Wang, M.-C. Tang, S. Chen, L. Li, D. Li, K.-Z. Hu, and M. Li, "Design of low-cost, flexible, uniplanar, electrically small, quasi-isotropic antenna," *IEEE Antennas Wireless Propag. Lett.*, vol. 18, no. 8, pp. 1646–1650, Aug. 2019.

[38] C. M. Kruesi, R. J. Vyas, and M. M. Tentzeris, "Design and development of a novel 3-D cubic antenna for wireless sensor networks (WSNs) and RFID applications," *IEEE Trans. Antennas Propag.*, vol. 57, no. 10, pp. 3293–3299, Oct. 2009.

[39] J. W. Luo, Y. M. Pan, S. Y. Zheng, and S. H. Wang, "A planar angled-dipole antenna with quasi-isotropic radiation pattern," *IEEE Trans. Antennas Propag.*, vol. 68, no. 7, pp. 5646–5651, Jul. 2020.

[40] Z. N. Chen, X. Qing, T. S. P. See, and W. K. Toh, "Antennas for WiFi connectivity," *Proc. IEEE*, vol. 100, no. 7, pp. 2322–2329, Jul. 2012.

[41] D. Psychogiou and J. Hesselbarth, "Diversity antennas for isotropic coverage," in *Proc. 3rd Eur. Wireless Technol. Conf.*, 2010, pp. 101–104.

[42] E. S. Pires, G. Fontgalland, M. A. B. de Melo, R. M. Valle, G. F. Aregao, and T. P. Vuong, "A new quasi-isotropic antenna for ultra-wideband application," in *IEEE MTT-S Int. Microw. Symp. Dig.*, Oct. 2007, pp. 100–103.

[43] L. A. Berge and M. T. Reich, "A UHF RFID antenna for a wireless sensor platform with a near-isotropic radiation pattern," in *Proc. IEEE Int. Conf. RFID (RFID)*, Apr. 2013, pp. 88–95.

[44] S. X. Ta, I. Park, and R. W. Ziolkowski, "Crossed dipole antennas: A review," *IEEE Antennas Propag. Mag.*, vol. 57, no. 5, pp. 107–122, Oct. 2015, doi: 10.1109/MAP.2015.2470680.

[45] R. Guertler, "Isotropic transmission-line antenna and its toroid-pattern modification," *IEEE Trans. Antennas Propag.*, vol. AP-25, no. 3, pp. 386–392, May 1977.

[46] E. da S. Pires, G. Fontgalland, R. M. do Valle, G. F. Aragao, W. R. N. Santos, and T. P. Vuong, "Proposal of a new compact isotropic antenna," in *Proc. IEEE Int. Symp. Electromagn. Compat.*, Jun. 2006, pp. 125–128.

[47] O. Yurtsev, Y. Bobkov, and S. Baty, "Several novel wire antenna designs with the quasi-isotropic radiation patterns in horizontal plane," in *Proc. VIII Int. Conf. Antenna Theory Techn.*, Sep. 2011, pp. 217–219.

[48] Z.-J. Tang, Y.-G. He, and Y. Wang, "Broadband UHF RFID tag antenna with quasi-isotropic radiation performance," *AEU-Int. J. Electron. Commun.*, vol. 65, no. 10, pp. 859–863, Oct. 2011, doi: 10.1016/j.aeue.2011.02.005.

[49] S. Lee, H. Jung, H. Choo, and I. Park, "Design of a U-shaped RFID tag antenna with an isotropic radiation characteristic," in *Proc. Int. Workshop Antenna Technol. (iWAT)*, Oct. 2011, pp. 306–309, doi: 10.1109/IWAT.2011.5752362.

[50] Y. M. Penkin and R. I. Klimovich, "Characteristics of quasi-isotropic radiators located on a semi-spherical protuberance on the screen," in *Proc. 4th Int. Kharkov Symp. Phys. Eng. Millim. Sub-Millim. Waves. Symp. Process.*, 1999, pp. 190–192, doi: 10.1109/MSMW.2001.946781.

[51] C. Cho, H. Choo, and I. Park, "Broadband RFID tag antenna with quasi-isotropic radiation pattern," *Electron. Lett.*, vol. 41, no. 20, p. 1091, 2005, doi: 10.1049/el:20052337.

[52] J. Singh, A. Modiri, and K. Kiasaleh, "Novel UWB hybrid dipole antenna with quasi-isotropic radiation pattern," in *Proc. IEEE Radio Wireless Symp.*, Jan. 2013, pp. 124–126, doi: 10.1109/RWS.2013.6486662.

[53] C.-H. Wu and T.-G. Ma, "Miniaturized self-oscillating active integrated antenna with quasi-isotropic radiation," *IEEE Trans. Antennas Propag.*, vol. 62, no. 2, pp. 933–936, Feb. 2014, doi: 10.1109/TAP.2013.2289942.

[54] S. Zhen and A. Shamim, "A 3D printed dual GSM band near isotropic on-package antenna," in *Proc. IEEE Int. Symp. Antennas Propag. USNC/URSI Nat. Radio Sci. Meeting*, Jul. 2017, pp. 1251–1252, doi: 10.1109/APUSNCURSINRSM.2017.8072668.

[55] P. Liu and Y. Li, "Quasi-isotropic radiation pattern synthesis using triple current line sources," *IEEE Trans. Antennas Propag.*, vol. 68, no. 12, pp. 8150–8155, Dec. 2020, doi: 10.1109/tap.2020.2995299.

[56] S. M. Radha, G. Shin, W. Kim, S. I. H. Shah, and I.-J. Yoon, "Design and verification of an electrically small, extremely thin dual-band quasi-isotropic antenna," *IEEE Antennas Wireless Propag. Lett.*, vol. 19, no. 12, pp. 2482–2486, Dec. 2020, doi: 10.1109/LAWP.2020.3036843.

[57] M. Arrawatia, M. S. Baghini, and G. Kumar, "Broadband modified elliptical ring quasi-isotropic antenna," in *Proc. IEEE Int. Symp. Antennas Propag. USNC/URSI Nat. Radio Sci. Meeting*, Jul. 2018, pp. 1055–1056, doi: 10.1109/APUSNCURSINRSM.2018.8608265.

[58] M. Dashti Ardakani and M. Tabatabaefar, "A transparent robust quasi-isotropic circularly polarized antenna for Cub-Sat and outdoor wireless," *Eng. Rep.*, vol. 2, no. 8, 2020, Art. no. e12224.

[59] R. C. Hall and D. I. Wu, "Modeling and design of circularly-polarized cylindrical wraparound microstrip antennas," in *Proc. Int. Symp. Antennas Propag.*, 1996, pp. 672–675, doi: 10.1109/APS.1996.549685.

[60] Z. Su, K. Klionovski, H. Liao, Y. Chen, A. Z. Elsherbeni, and A. Shamim, "Antenna-on-package design: Achieving near-isotropic radiation pattern and wide CP coverage simultaneously," *IEEE Trans. Antennas Propag.*, vol. 69, no. 7, pp. 3740–3749, Jul. 2021, doi: 10.1109/TAP.2020.3044134.

[61] D. L. Wu, "Omnidirectional circularly-polarized conformal microstrip array for telemetry applications," in *Proc. Int. Symp. Antennas Propag. Soc.*, vol. 2, Oct. 1995, pp. 998–1001, doi: 10.1109/APS.1995.530185.

[62] A. Erentok and R. W. Ziolkowski, "Metamaterial-inspired efficient electrically small antennas," *IEEE Trans. Antennas Propag.*, vol. 56, no. 3, pp. 691–707, Mar. 2008, doi: 10.1109/TAP.2008.916949.

[63] S. Imran Hussain Shah, M. M. Tentzeris, and S. Lim, "Planar quasi-isotropic antenna for drone communication," *Microw. Opt. Technol. Lett.*, vol. 60, no. 5, pp. 1290–1295, May 2018.

[64] M. F. Farooqui, C. Claudel, and A. Shamim, "An inkjet-printed buoyant 3-D lagrangian sensor for real-time flood monitoring," *IEEE Trans. Antennas Propag.*, vol. 62, no. 6, pp. 3354–3359, Jun. 2014, doi: 10.1109/TAP.2014.2309957.

[65] Q. Zhang, Y.-H. Kuo, N. Mishra, and A. Shamim, "Flexible quasi-isotropic antenna for marine animals tagging application," in *Proc. Int. Flexible Electron. Technol. Conf. (IFETC)*, Aug. 2018, pp. 1–10, doi: 10.1109/IFETC.2018.8583987.

[66] C. Balanis, *Antenna Theory: Analysis and Design*, vol. 1. Hoboken, NJ, USA: Wiley, 2005.

[67] I. Jayakumar, R. Garg, B. Sarap, and B. Lal, "A conformal cylindrical microstrip array for producing omnidirectional radiation pattern," *IEEE Trans. Antennas Propag.*, vol. AP-34, no. 10, pp. 1258–1261, Oct. 1986, doi: 10.1109/TAP.1986.1143743.

[68] S. Junhao, "A printed dipole array for omni directional application," in *Proc. 8th Int. Symp. Antennas, Propag. EM Theory*, 2008, pp. 182–184, doi: 10.1109/ISAPE.2008.4735171.

[69] Q. Jinghui, Z. Lingling, D. Hailong, L. Wei, Q. Jinghui, Z. Lingling, D. Hailong, and L. Wei, "Analysis and simulation of cylindrical conformal omnidirectional antenna," in *Proc. Asia–Pacific Microw. Conf. Proc.*, 2005, ppp. 1–4, doi: 10.1109/APMC.2005.1606841.

[70] G. Dubost, J. Samson, and R. Frin, "Large-bandwidth flat cylindrical array with circular polarisation and omnidirectional radiation," *Electron. Lett.*, vol. 15, no. 4, p. 102, 1979, doi: 10.1049/el:19790074.

[71] D. K. Naji, "Miniature slotted semi-circular dual-band antenna for Wimax and WLAN applications," *J. Electromagn. Eng. Sci.*, vol. 20, no. 2, pp. 115–124, Apr. 2020, doi: 10.26866/JEES.2020.20.2.115.

[72] S. L. Gunamony, J. B. Gnanadhas, and D. E. Lawrence, "Design and investigation of a miniaturized single-layer ACS-fed dual band antenna for LTE and 5G applications," *J. Electromagn. Eng. Sci.*, vol. 20, no. 3, pp. 213–220, Jul. 2020, doi: 10.26866/JEES.2020.20.3.213.

[73] Y. Dong and T. Itoh, "Metamaterial-inspired broadband mushroom antenna," in *Proc. IEEE Antennas Propag. Soc. Int. Symp.*, Jul. 2010, pp. 1–4, doi: 10.1109/APS.2010.5560998.

[74] K. E. Kedze, H. Wang, and I. Park, "Effects of split position on the performance of a compact broadband printed dipole antenna with split-ring resonators," *J. Electromagn. Eng. Sci.*, vol. 19, no. 2, pp. 115–121, Apr. 2019, doi: 10.26866/JEES.2019.19.2.115.

[75] A. Ali, H. Wang, Y. Yun, J. Lee, and I. Park, "Compact slot antenna integrated with a photovoltaic cell," *J. Electromagn. Eng. Sci.*, vol. 20, no. 4, pp. 248–253, Oct. 2020, doi: 10.26866/jees.2020.20.4.248.
[76] Y. Dong and T. Itoh, "Metamaterial-based antennas," *Proc. IEEE*, vol. 100, no. 7, pp. 2271–2285, Jul. 2012, doi: 10.1109/JPROC.2012.2187631.
[77] H. Nakano, J. Miyake, M. Oyama, and J. Yamauchi, "Metamaterial spiral antenna," *IEEE Antennas Wireless Propag. Lett.*, vol. 10, pp. 1555–1558, 2011, doi: 10.1109/LAWP.2011.2181305.
[78] H. Mirzaei and G. V. Eleftheriades, "A compact frequency-reconfigurable metamaterial-inspired antenna," *IEEE Antennas Wireless Propag. Lett.*, vol. 10, pp. 1154–1157, 2011, doi: 10.1109/LAWP.2011.2172180.
[79] F. Bilotti and L. Vegni, "From metamaterial-based to metamaterial-inspired miniaturized antennas: A possible procedure and some examples," in *Proc. URSI Gen. Assem. Process.*, 2008, pp. 1–4.
[80] R. Wang, J.-J. Ma, C.-S. Chen, B.-Z. Wang, and J. Xiong, "Low-profile implementation of U-shaped power quasi-isotropic antennas for intra-vehicle wireless communications," *IEEE Access*, vol. 8, pp. 48557–48565, 2020, doi: 10.1109/ACCESS.2020.2979880.

SYED IMRAN HUSSAIN SHAH received the B.Sc. degree in telecommunication engineering and the M.S. degree in electrical engineering from the University of Engineering and Technology, Peshawar, Pakistan, in 2011 and 2014, respectively, and the Ph.D. degree from the School of Electrical and Electronics Engineering, Chung-Ang University, Seoul, Republic of Korea, in 2020. Since August 2020, he has been working as a Postdoctoral Researcher at Chungnam National University, Daejeon, Republic of Korea. He has authored more than 30 journals and conference papers focused on reconfigurable, deployable, printed smart antennas, and quasi-isotropic antennas. His research interests include the design and analysis of frequency and pattern reconfigurable origami antennas, deployable origami antennas, 3-D printed antennas, and shape memory materials-based smart antennas.

SONAPREETHA MOHAN RADHA (Student Member, IEEE) received the B.S. degree in electronics and communication engineering from Anna University, Chennai, India, in 2012, and the M.S. degree in nuclear and quantum engineering from the Korea Advanced Institute of Science and Technology (KAIST), Daejeon, Republic of Korea, in 2016. She is currently pursuing the Ph.D. degree in electrical engineering with Chungnam National University, Daejeon. Her research interests include electrically small antennas, electromagnetic compatibility, and metamaterial and wireless power transfer.

PANGUN PARK (Member, IEEE) received the M.S. and Ph.D. degrees in electrical engineering from the Royal Institute of Technology, Sweden, in 2007 and 2011, respectively. From 2011 to 2013, he has held a postdoctoral research position in electrical engineering and computer science from the University of California at Berkeley, Berkeley, CA, USA. He is currently an Associate Professor with the Department of Radio and Information Communications Engineering, Chungnam National University, Daejeon, South Korea.

ICK-JAE YOON (Senior Member, IEEE) received the B.S. and M.S. degrees from Yonsei University, Seoul, Republic of Korea, in 2003 and 2005, respectively, and the Ph.D. degree from The University of Texas at Austin, Austin, TX, USA, in 2012, all in electrical engineering. From 2005 to 2008, he worked as a Research Engineer at Samsung Advanced Institute of Technology, Samsung Electronics Company, Yongin, Republic of Korea. From 2012 to 2014, he was with the Electromagnetic Systems Group, Department of Electrical Engineering, Technical University of Denmark (DTU), Lyngby, Denmark, as a Postdoctoral Research Fellow and an Assistant Professor. He joined the Faculty of Chungnam National University, Daejeon, Republic of Korea, in 2014, where he is currently an Associate Professor with the Department of Electrical Engineering. His current research interests include antennas, RF/microwave circuits, electromagnetic compatibility, and theoretical methods for electromagnetics. He received the H. C. Ørsted Postdoctoral Fellowship from DTU, in 2012.